

See discussions, stats, and author profiles for this publication at: <https://www.researchgate.net/publication/11884473>

# Synthesis, Structures, and Reactivity of Weakly Coordinating Anions with Delocalized Borate Structure: The Assessment of Anion Effects in Metallocene Polymerization Catalysts

ARTICLE in JOURNAL OF THE AMERICAN CHEMICAL SOCIETY · FEBRUARY 2001

Impact Factor: 12.11 · DOI: 10.1021/ja002820h · Source: PubMed

CITATIONS

170

READS

38

## 6 AUTHORS, INCLUDING:



[Simon J. Lancaster](#)

University of East Anglia

68 PUBLICATIONS 2,556 CITATIONS

[SEE PROFILE](#)



[Stefan Beck](#)

Synthes Holding AG

20 PUBLICATIONS 705 CITATIONS

[SEE PROFILE](#)



[M. Thornton-Pett](#)

Botany Downs Secondary College, Auckland, ...

474 PUBLICATIONS 7,999 CITATIONS

[SEE PROFILE](#)



[Manfred Bochmann](#)

University of East Anglia

302 PUBLICATIONS 8,996 CITATIONS

[SEE PROFILE](#)

# Synthesis, Structures, and Reactivity of Weakly Coordinating Anions with Delocalized Borate Structure: The Assessment of Anion Effects in Metallocene Polymerization Catalysts

Jiamin Zhou, Simon J. Lancaster,<sup>†</sup> Dennis A. Walker,<sup>†</sup> Stefan Beck,<sup>†</sup> Mark Thornton-Pett, and Manfred Bochmann<sup>\*,†</sup>

Contribution from the School of Chemistry, University of Leeds, Leeds LS2 9JT, U.K.

Received July 31, 2000

**Abstract:** The formation of adducts of tris(pentafluorophenyl)borane with strongly coordinating anions such as CN<sup>−</sup> and [M(CN)<sub>4</sub>]<sup>2−</sup> (M = Ni, Pd) is a synthetically facile route to the bulky, very weakly coordinating anions [CN{B(C<sub>6</sub>F<sub>5</sub>)<sub>3</sub>}<sub>2</sub>]<sup>−</sup> and [M{CNB(C<sub>6</sub>F<sub>5</sub>)<sub>3</sub>}<sub>4</sub>]<sup>2−</sup> which are isolated as stable NHMe<sub>2</sub>Ph<sup>+</sup> and CPh<sub>3</sub><sup>+</sup> salts. The crystal structures of [CPh<sub>3</sub>][CN{B(C<sub>6</sub>F<sub>5</sub>)<sub>3</sub>}<sub>2</sub>] (**1**), [CPh<sub>3</sub>][CIB(C<sub>6</sub>F<sub>5</sub>)<sub>3</sub>] (**2**), [NHMe<sub>2</sub>Ph]<sub>2</sub>[Ni{CNB(C<sub>6</sub>F<sub>5</sub>)<sub>3</sub>}<sub>4</sub>]·2Me<sub>2</sub>CO (**4b**·2Me<sub>2</sub>CO), [CPh<sub>3</sub>]<sub>2</sub>[Ni{CNB(C<sub>6</sub>F<sub>5</sub>)<sub>3</sub>}<sub>4</sub>]·2CH<sub>2</sub>Cl<sub>2</sub> (**4c**·2CH<sub>2</sub>Cl<sub>2</sub>), and [CPh<sub>3</sub>]<sub>2</sub>[Pd{CNB(C<sub>6</sub>F<sub>5</sub>)<sub>3</sub>}<sub>4</sub>]·2CH<sub>2</sub>Cl<sub>2</sub> (**5c**·2CH<sub>2</sub>Cl<sub>2</sub>) are reported. The CN stretching frequencies in **4** and **5** are shifted by ~110 cm<sup>−1</sup> to higher wavenumbers compared to the parent tetracyano complexes in aqueous solution, although the M–C and C–N distances show no significant change on B(C<sub>6</sub>F<sub>5</sub>)<sub>3</sub> coordination. Zirconocene dimethyl complexes L<sub>2</sub>ZrMe<sub>2</sub> [L<sub>2</sub> = Cp<sub>2</sub>, SBI = *rac*-Me<sub>2</sub>Si(Ind)<sub>2</sub>] react with **1**, **4c** or **5c** in benzene solution at 20 °C to give the salts of binuclear methyl-bridged cations, [(L<sub>2</sub>ZrMe)<sub>2</sub>(μ-Me)][CN{B(C<sub>6</sub>F<sub>5</sub>)<sub>3</sub>}<sub>2</sub>] and [(L<sub>2</sub>ZrMe)<sub>2</sub>(μ-Me)]<sub>2</sub>[M{CNB(C<sub>6</sub>F<sub>5</sub>)<sub>3</sub>}<sub>4</sub>]. The reactivity of these species in solution was studied in comparison with the known [(SBI)ZrMe]<sub>2</sub>(μ-Me)[B(C<sub>6</sub>F<sub>5</sub>)<sub>4</sub>]. While the latter reacts with excess [CPh<sub>3</sub>][B(C<sub>6</sub>F<sub>5</sub>)<sub>4</sub>] in benzene to give the mononuclear ion pair [(SBI)ZrMe<sup>+</sup>...B(C<sub>6</sub>F<sub>5</sub>)<sub>4</sub><sup>−</sup>] in a pseudo-first-order reaction, *k* = 3 × 10<sup>−4</sup> s<sup>−1</sup>, [(L<sub>2</sub>ZrMe)<sub>2</sub>(μ-Me)][CN{B(C<sub>6</sub>F<sub>5</sub>)<sub>3</sub>}<sub>2</sub>] reacts to give a mixture of L<sub>2</sub>ZrMe(μ-Me)B(C<sub>6</sub>F<sub>5</sub>)<sub>3</sub> and L<sub>2</sub>ZrMe(μ-NC)B(C<sub>6</sub>F<sub>5</sub>)<sub>3</sub>. Recrystallization of [Cp''<sub>2</sub>Zr(μ-Me)<sub>2</sub>AlMe<sub>2</sub>][CN{B(C<sub>6</sub>F<sub>5</sub>)<sub>3</sub>}<sub>2</sub>] affords Cp''<sub>2</sub>ZrMe(μ-NC)B(C<sub>6</sub>F<sub>5</sub>)<sub>3</sub> **6**, the X-ray structure of which is reported. The stability of [(L<sub>2</sub>ZrMe)<sub>2</sub>(μ-Me)]<sup>+</sup>X<sup>−</sup> decreases in the order X = [B(C<sub>6</sub>F<sub>5</sub>)<sub>4</sub>]<sup>−</sup> > [M{CNB(C<sub>6</sub>F<sub>5</sub>)<sub>3</sub>}<sub>4</sub>]<sup>2−</sup> > [CN{B(C<sub>6</sub>F<sub>5</sub>)<sub>3</sub>}<sub>2</sub>]<sup>−</sup> and increases strongly with the steric bulk of L<sub>2</sub> = Cp<sub>2</sub> ≪ SBI. Activation of (SBI)ZrMe<sub>2</sub> by **1** in the presence of AlBu<sub>3</sub> gives extremely active ethene polymerization catalysts. Polymerization studies at 1–7 bar monomer pressure suggest that these, and by implication most other highly active ethene polymerization catalysts, are strongly mass-transport limited. By contrast, monitoring propene polymerization activities with the systems (SBI)ZrMe<sub>2</sub>/1/AlBu<sub>3</sub> and CGCTiMe<sub>2</sub>/1/AlBu<sub>3</sub> at 20 °C as a function of catalyst concentration demonstrates that in these cases mass-transport limitation is absent up to [metal] ≈ 2 × 10<sup>−5</sup> mol L<sup>−1</sup>. Propene polymerization activities decrease in the order [CN{B(C<sub>6</sub>F<sub>5</sub>)<sub>3</sub>}<sub>2</sub>]<sup>−</sup> > [B(C<sub>6</sub>F<sub>5</sub>)<sub>4</sub>]<sup>−</sup> > [M{CNB(C<sub>6</sub>F<sub>5</sub>)<sub>3</sub>}<sub>4</sub>]<sup>2−</sup> ≫ [MeB(C<sub>6</sub>F<sub>5</sub>)<sub>3</sub>]<sup>−</sup>, with differences in activation barriers relative to [CN{B(C<sub>6</sub>F<sub>5</sub>)<sub>3</sub>}<sub>2</sub>]<sup>−</sup> of ΔΔ*G*<sup>‡</sup> = 1.1 (B(C<sub>6</sub>F<sub>5</sub>)<sub>4</sub><sup>−</sup>), 4.1 (Ni{CNB(C<sub>6</sub>F<sub>5</sub>)<sub>3</sub>}<sub>4</sub><sup>2−</sup>) and 10.7–12.8 kJ mol<sup>−1</sup> (MeB(C<sub>6</sub>F<sub>5</sub>)<sub>3</sub><sup>−</sup>). The data suggest that even in the case of very bulky anions with delocalized negative charge the displacement of the anion by the monomer must be involved in the rate-limiting step.

## Introduction

The profound effect of counteranions on the reactivity and catalytic activity of cationic early transition-metal complexes is well-established.<sup>1–4</sup> For example, while BPh<sub>4</sub><sup>−</sup> has a tendency to form π-complexes and tight ion pairs,<sup>5</sup> the weak coordinating ability of its perfluoro analogue [B(C<sub>6</sub>F<sub>5</sub>)<sub>4</sub>]<sup>−</sup> and its congeners

leads to a dramatic increase in activity and is the basis of the use of ionic systems [L<sub>n</sub>MR]<sup>+</sup>[R'B(ArF)<sub>3</sub>]<sup>−</sup> as highly effective olefin polymerization catalysts.<sup>6</sup> In particular, Marks has demonstrated that suitable elaboration of the perfluoroaryl borate counteranion can result in significant enhancements in stability and activity of ionic metallocene catalysts.<sup>7,8</sup> However, in view of the fact that the preparation of such anions is costly and involves not insignificant synthetic effort, we have become

\* To whom correspondence should be addressed. E-mail: m.bochmann@uea.ac.uk. Fax: +44 1603 592044.

<sup>†</sup> Current address: School of Chemical Sciences, University of East Anglia, Norwich NR4 7TJ, UK.

(1) (a) Lupinetti, A. J.; Strauss, S. H. *Chemtracts: Inorg. Chem.* **1998**, *11*, 565. (b) Reed, C. A. *Acc. Chem. Res.* **1998**, *31*, 133. (c) Strauss, S. H. *Chem. Rev.* **1993**, *93*, 927.

(2) (a) Bochmann, M.; Jaggard, A. J. *J. Organomet. Chem.* **1992**, *424*, C5. (b) Bochmann, M. *Angew. Chem., Int. Ed. Engl.* **1992**, *31*, 1181.

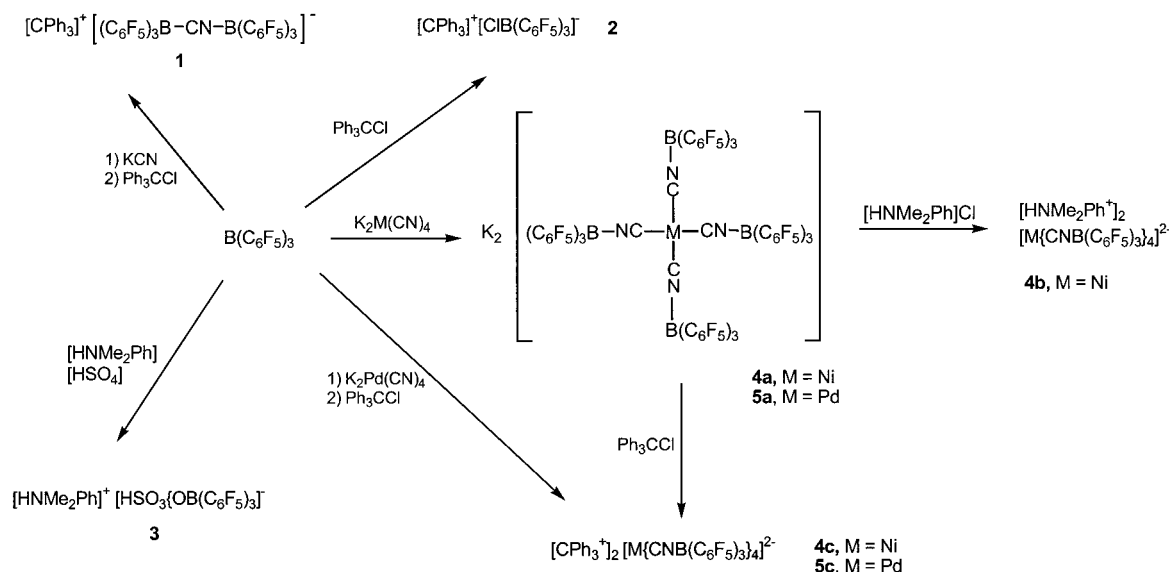
(3) Yang, X.; Stern, C. L.; Marks, T. J. *Organometallics* **1991**, *10*, 840.

(4) (a) Siedle, A. R.; Lamanna, W. M.; Newmark, R. A.; Stevens, J.; Richardson, D. E.; Ryan, M. *Makromol. Chem., Macromol. Symp.* **1993**, *66*, 215. (b) Chien, J. C. W.; Song, W.; Rausch, M. D. *J. Polym. Sci., Part A: Polym. Chem.* **1994**, *32*, 2387.

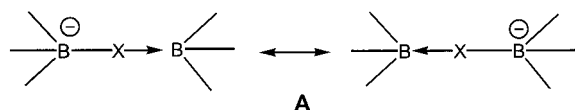
(5) See, for example: (a) Bochmann, M.; Karger, G.; Jaggard, A. J. *J. Chem. Soc., Chem. Commun.* **1990**, 1038. (b) Horton, A. D.; Frijns, J. H. *G. Angew. Chem., Int. Ed. Engl.* **1991**, *30*, 1152. (c) Schaverien, C. J. *Organometallics* **1992**, *11*, 3476. (d) Calderazzo, F.; Englert, U.; Pampaloni, G.; Rocchi, L. *Angew. Chem., Int. Ed. Engl.* **1992**, *31*, 1235. (e) Solari, E.; Musso, F.; Gallo, E.; Floriani, C.; Re, N.; Chiesi-Villa, A.; Rizzoli, C. *Organometallics* **1995**, *14*, 2265.

(6) Turner, H. W. Eur. Patent Appl. 0277 004, 1988. (b) Ewen, J. A.; Elder, M. J. Eur. Patent Appl. 0426 637, 1990. (c) Ewen, J. A.; Elder, M. J. Eur. Patent Appl. 0427 697, 1991. (d) Yang, X.; Stern, C. L.; Marks, T. J. *J. Am. Chem. Soc.* **1991**, *113*, 3623. (e) Ewen, J. A.; Elder, M. J. *Makromol. Chem., Macromol. Symp.* **1993**, *66*, 179. (f) Ewen, J. A. *Stud. Surf. Sci. Catal.* **1994**, *89*, 405.

## Scheme 1



interested in methods of generating new bulky anions in a more straightforward manner. One such method is the facile adduct formation between commercially available  $\text{B}(\text{C}_6\text{F}_5)_3$  and strongly coordinating anions.<sup>10</sup> With this aim in mind we have recently reported the synthesis of  $[\text{CPh}_3][\text{CN}\{\text{B}(\text{C}_6\text{F}_5)_3\}_2]$  (**1**) and  $[\text{CPh}_3]_2[\text{Ni}\{\text{CNB}(\text{C}_6\text{F}_5)_3\}_4]$  (**4c**) and their use as activators for zirconocene-based ethene polymerization catalysts in a preliminary communication.<sup>11</sup> In contrast to borates of the type  $[\text{R}'\text{B}(\text{Ar}_\text{F})_3]^-$  and  $[\text{B}(\text{Ar}_\text{F})_3]^-$ , which contain one negative charge per boron atom, the charge in the oligoborates **1** and **4** is delocalized and reduced to 0.5/B (structure A). Both for steric



and electronic reasons it seemed reasonable to expect that as counterions for cationic early transition-metal catalysts such

(7) (a) Jia, L.; Yang, X.; Ishihara, A.; Marks, T. J. *Organometallics* **1995**, 14, 3135. (b) Chen, Y. X.; Stern, C. L.; Yang, S.; Marks, T. J. *J. Am. Chem. Soc.* **1996**, 118, 12451. (c) Jia, L.; Yang, X.; Stern, C. L.; Marks, T. J. *Organometallics* **1997**, 16, 842. (d) Chen, Y. X.; Marks, T. J. *Organometallics* **1997**, 16, 3649. (e) Chen, Y. X.; Stern, C. L.; Marks, T. J. *J. Am. Chem. Soc.* **1997**, 119, 2582. (f) Chen, Y. X.; Metz, M. V.; Li, L.; Stern, C. L.; Marks, T. J. *J. Am. Chem. Soc.* **1998**, 120, 6287. (g) Li, L.; Marks, T. J. *Organometallics* **1998**, 17, 3996. (h) Metz, M. V.; Schwartz, D. J.; Stern, C. L.; Nickias, P. N.; Marks, T. J. *Angew. Chem., Int. Ed.* **2000**, 39, 1312. (i) Chen, E. Y. X.; Marks, T. J. *Chem. Rev.* **2000**, 100, 1391.

(8) For related boranes, see: (a) Köhler, K.; Piers, W. E. *Can. J. Chem.* **1998**, 76, 1249. (b) Köhler, K.; Piers, W. E.; Jarvis, A. P.; Xin, S.; Feng, Y.; Brasakis, A. M.; Collins, S.; Clegg, W.; Yap, G. P. A.; Marder, T. B. *Organometallics* **1998**, 17, 3557. (c) Williams, V. C.; Piers, W. E.; Clegg, W.; Elsegood, M. R. J.; Collins, S.; Marder, T. B. *J. Am. Chem. Soc.* **1999**, 121, 3244. (d) Williams, V. C.; Dai, C.; Li, Z.; Collins, S.; Piers, W. E.; Clegg, W.; Elsegood, M. R. J.; Marder, T. B. *Angew. Chem., Int. Ed.* **1999**, 38, 3695. (e) Williams, V. C.; Irvine, G. J.; Piers, W. E.; Li, Z.; Collins, S.; Clegg, W.; Elsegood, M. R. J.; Marder, T. B. *Organometallics* **2000**, 19, 1619.

(9) (a) Massey, A. G.; Park, A. J.; Stone, F. G. A. *Proc. Chem. Soc. [London]* **1963**, 212. (b) Massey, A. G.; Park, A. J. *J. Organomet. Chem.* **1964**, 2, 245. (c) Pohlmann, J. L. W.; Brinckmann, F. E. *Z. Naturforsch. B* **1965**, 20b, 5.

(10) Anions derived from adducts between  $\text{B}(\text{C}_6\text{F}_5)_3$  and alcohols, silanols and oximes and their use in polymerization catalysis are known: Siedle, A. R.; Lamanna, W. M. U.S. Patent 5,416,177, 1995 and ref 4a.

(11) (a) Lancaster, S. J.; Walker, D. A.; Thornton-Pett, M.; Bochmann, M. *Chem. Commun.* **1999**, 1533. (b) Compound **1** and related anions have been independently reported in a patent: LaPointe, R. E. WO 99/42467, 1999.

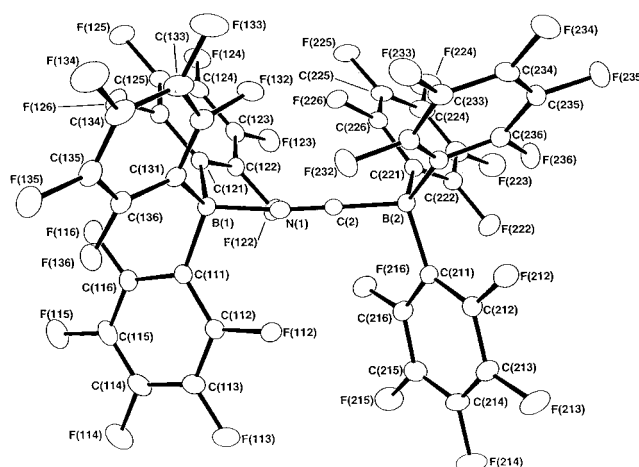


**Figure 1.** Structure of the  $[\text{CN}\{\text{B}(\text{C}_6\text{F}_5)_3\}_2]^-$  anion in **1**, showing the atomic numbering scheme. Ellipsoids are drawn at 40% probability level.

anions would show reduced ion pairing and hence increased catalytic activity. Preliminary results with (SBI)ZrMe<sub>2</sub>/1 mixtures (SBI = *rac*-Me<sub>2</sub>Si(Ind)<sub>2</sub>) indicated that this expectation was justified.<sup>11a</sup> We report here the evaluation of oligoborates as activators in high-activity ethene and propene polymerization catalysts.

## Results

**Anion Synthesis.** Stirring a suspension of KCN with 2 equiv of  $\text{B}(\text{C}_6\text{F}_5)_3 \cdot \text{Et}_2\text{O}$  in diethyl ether at room temperature for 12 h leads to the slow dissolution of the solid to give a clear solution. Replacing the ether solvent with dichloromethane and adding 1 equiv of chlorotriphenylmethane gives an orange-yellow solution from which  $[\text{CPh}_3][\text{CN}\{\text{B}(\text{C}_6\text{F}_5)_3\}_2]$  (**1**) is isolated in 45% yield (Scheme 1). Crystalline **1** is not affected by storing in air at ambient conditions for extended periods of time. Crystals suitable for X-ray diffraction were grown from dichloromethane/light petroleum mixtures. The structure is shown in Figure 1, and selected bond lengths and angles are given in Table 1. The CN-bridged geometry is further confirmed by the observation of two <sup>11</sup>B NMR signals at  $\delta$  -11.94 and -21.68 and the  $\nu_{\text{CN}}$  stretching frequency at 2305 cm<sup>-1</sup>. Structurally related cyanoborates are known, viz.  $[\text{CN}(\text{BH}_3)_2]^-$  and  $[\text{CN}-$

**Table 1.** Selected Bond Distances [Å] and Angles [deg]

[CPh <sub>3</sub> ][CN{B(C <sub>6</sub> F <sub>5</sub> ) <sub>3</sub> } <sub>2</sub> ] <b>1</b>	
B(1)–N(1) 1.593(2)	B(2)–C(2) 1.583(2)
C(2)–N(1) 1.144(2)	B(1)–C(111) 1.1636(2)
B(1)–C(121) 1.1646(2)	B(1)–C(131) 1.1644(2)
C(2)–N(1)–B(1) 173.55(14)	N(1)–C(2)–B(2) 174.50(14)
N(1)–B(1)–C(111) 108.41(11)	N(1)–B(1)–C(121) 103.71(11)
N(1)–B(1)–C(131) 104.75(11)	C(111)–B(1)–C(121) 111.02(11)
[CPh <sub>3</sub> ][CIB(C <sub>6</sub> F <sub>5</sub> ) <sub>3</sub> ] <b>2</b>	
B–Cl 1.928(2)	B–C(11) 1.646(3)
B–C(21) 1.649(3)	B–C(31) 1.648(3)
C(11)–B–Cl 105.10(14)	C(21)–B–Cl 111.69(14)
C(31)–B–Cl 103.31(14)	C(11)–B–C(21) 107.7(2)
C(11)–B–C(31) 115.5(2)	C(21)–B–C(31) 113.2(2)
[HNMe <sub>2</sub> Ph] <sub>2</sub> [Ni{CNB(C <sub>6</sub> F <sub>5</sub> ) <sub>3</sub> } <sub>4</sub> ]·2Me <sub>2</sub> CO <b>4b</b>	
Ni–C(1) 1.851(2)	Ni–C(2) 1.856(2)
C(1)–N(1) 1.143(3)	N(1)–B(1) 1.582(3)
C(2)–N(2) 1.143(3)	N(2)–B(2) 1.578(3)
B(1)–C(111) 1.636(3)	B(1)–C(121) 1.639(3)
C(1)–Ni–C(1)* 180.0	C(1)–Ni–C(2)* 89.44(9)
C(1)–Ni–C(2) 90.56(9)	N(1)–C(1)–Ni 178.3(2)
N(2)–C(2)–Ni 174.8(2)	C(1)–N(1)–B(1) 177.5(2)
C(2)–N(2)–B(2) 178.2(2)	N(1)–B(1)–C(111) 105.9(2)
[CPh <sub>3</sub> ] <sub>2</sub> [Ni{CNB(C <sub>6</sub> F <sub>5</sub> ) <sub>3</sub> } <sub>4</sub> ]·2CH <sub>2</sub> Cl <sub>2</sub> <b>4c</b>	
Ni–C(1) 1.855(2)	Ni–C(2) 1.862(2)
C(1)–N(1) 1.145(2)	N(1)–B(1) 1.574(2)
C(2)–N(2) 1.146(2)	N(2)–B(2) 1.574(2)
B(1)–C(111) 1.635(3)	B(1)–C(121) 1.642(3)
C(1)–Ni–C(1)* 180.0	C(1)–Ni–C(2)* 92.85(7)
C(1)–Ni–C(2) 87.15(7)	N(1)–C(1)–Ni 176.5(2)
N(2)–C(2)–Ni 175.2(2)	C(1)–N(1)–B(1) 174.8(2)
C(2)–N(2)–B(2) 175.6(2)	N(1)–B(1)–C(111) 103.65(14)
[CPh <sub>3</sub> ] <sub>2</sub> [Pd{CNB(C <sub>6</sub> F <sub>5</sub> ) <sub>3</sub> } <sub>4</sub> ]·2CH <sub>2</sub> Cl <sub>2</sub> <b>5c</b>	
Pd–C(1) 1.989(2)	Pd–C(2) 1.995(2)
C(1)–N(1) 1.126(3)	N(1)–B(1) 1.577(3)
C(2)–N(2) 1.126(3)	N(2)–B(2) 1.571(3)
B(1)–C(111) 1.639(3)	B(1)–C(121) 1.645(3)
C(1)–Pd–C(1)* 180.0(2)	C(1)–Pd–C(2)* 87.05(8)
C(1)–Pd–C(2) 92.95(8)	N(1)–C(1)–Pd 176.6(2)
N(2)–C(2)–Pd 174.7(2)	C(1)–N(1)–B(1) 175.3(2)
C(2)–N(2)–B(2) 175.5(2)	N(1)–B(1)–C(111) 106.4(2)
Cp'' <sub>2</sub> Zr(Me)NCB(C <sub>6</sub> F <sub>5</sub> ) <sub>3</sub> ·C <sub>7</sub> H <sub>8</sub> <b>6</b>	
Zr–C(14) 2.254(3)	Zr–N(1) 2.259(2)
N(1)–C(16) 1.149(3)	C(16)–B(1) 1.614(4)
B(1)–C(111) 1.639(4)	Zr–C(1) 2.508(3)
Zr–C(2) 2.511(3)	Zr–C(3) 2.530(2)
Zr–C(4) 2.496(3)	Zr–C(5) 2.486(3)
B(1)–C(111) 1.639(4)	C(1)–Si(1) 1.878(3)
C(14)–Zr–N(1) 102.60(10)	Zr–N(1)–C(16) 175.1(2)
N(1)–C(16)–B(1) 174.1(3)	C(16)–B(1)–C(111) 111.2(2)
C(16)–B(1)–C(121) 102.6(2)	C(16)–B(1)–C(131) 105.0(2)

(BPh<sub>3</sub>)<sub>2</sub>]<sup>–</sup>; they are characterized by closely similar  $\nu_{\text{CN}}$  frequencies (2305 and 2255 cm<sup>–1</sup>, respectively).<sup>12,13</sup> The latter was found to be prone to dissociation into BPh<sub>3</sub> and [Ph<sub>3</sub>BCN]<sup>–</sup>. In the case of the much stronger Lewis acid B(C<sub>6</sub>F<sub>5</sub>)<sub>3</sub> such a dissociation process appears to be disfavored.<sup>14</sup>

Oxo anions represent a weaker type of donors and form less stable complexes. Stirring a mixture of KNO<sub>3</sub>, Ph<sub>3</sub>CCl, and B(C<sub>6</sub>F<sub>5</sub>)<sub>3</sub>·Et<sub>2</sub>O in dichloromethane in a procedure analogous to

(12) Wade, R. C.; Sullivan, E. A.; Berscheid, J. R.; Purcell, K. F. *Inorg. Chem.* **1970**, *9*, 2146.

(13) Giandomenico, C. M.; Dewan, J. C.; Lippard, S. J. *J. Am. Chem. Soc.* **1991**, *113*, 1407.

(14) For a discussion of Lewis acid strengths of boranes see: Luo, L.; Marks, T. J. *Top. Catal.* **1999**, *7*, 97.

that used for **1** fails to give the nitrate adduct but generates [CPh<sub>3</sub>][CIB(C<sub>6</sub>F<sub>5</sub>)<sub>3</sub>] (**2**) in good yield. The same product is obtained in the absence of KNO<sub>3</sub>. The structure of **2** was confirmed by X-ray crystallography; the anion is identical to that obtained by Erker et al. from the reaction of (Ar<sub>2</sub>PCMe<sub>2</sub>-Cp)<sub>2</sub>ZrCl<sub>2</sub> and B(C<sub>6</sub>F<sub>5</sub>)<sub>3</sub> (Ar = *p*-tolyl).<sup>15</sup> By contrast, the reaction of [PhNMe<sub>2</sub>H][HSO<sub>4</sub>] with B(C<sub>6</sub>F<sub>5</sub>)<sub>3</sub>·Et<sub>2</sub>O in dichloromethane affords [PhNMe<sub>2</sub>H][HSO<sub>3</sub>{OB(C<sub>6</sub>F<sub>5</sub>)<sub>3</sub>}] (**3**).<sup>16</sup>

The tetracyanometalates [M(CN)<sub>4</sub>]<sup>2–</sup> are characterized by very high formation constants in aqueous solution, 10<sup>31</sup> for M = Ni and 10<sup>42</sup> – 10<sup>51.7</sup> given for M = Pd.<sup>17</sup> These anions therefore promised to produce very stable adducts with B(C<sub>6</sub>F<sub>5</sub>)<sub>3</sub>. Stirring a mixture of K<sub>2</sub>[Ni(CN)<sub>4</sub>] with B(C<sub>6</sub>F<sub>5</sub>)<sub>3</sub>·Et<sub>2</sub>O in dichloromethane did indeed give the expected product, K<sub>2</sub>[Ni{CNB(C<sub>6</sub>F<sub>5</sub>)<sub>3</sub>}<sub>4</sub>] (**4a**), as a white solid. Cation exchange with [NHMe<sub>2</sub>Ph]Cl afforded the corresponding dimethylanilinium salt **4b**, while the CPh<sub>3</sub><sup>+</sup> salt **4c** was made directly from Ph<sub>3</sub>CCl, K<sub>2</sub>[Ni(CN)<sub>4</sub>] and B(C<sub>6</sub>F<sub>5</sub>)<sub>3</sub>·Et<sub>2</sub>O. Crystals of **4b**·2Me<sub>2</sub>CO were grown from dichloromethane containing small amounts of acetone. The palladium compounds A<sub>2</sub>[Pd{CNB(C<sub>6</sub>F<sub>5</sub>)<sub>3</sub>}<sub>4</sub>] **5a**, (A = K) and **5c** (A = CPh<sub>3</sub>) were obtained by analogous procedures as crystalline solids.

Coordination of B(C<sub>6</sub>F<sub>5</sub>)<sub>3</sub> to [M(CN)<sub>4</sub>]<sup>2–</sup> significantly raises the C–N stretching frequencies. The nickel complexes **4** show infrared absorptions at ~2236 cm<sup>–1</sup>, essentially independent of the cation, compared to 2123.5 cm<sup>–1</sup> for K<sub>2</sub>Ni(CN)<sub>4</sub> in aqueous solution.<sup>18</sup> The corresponding frequency for the Pd complex **5c** is observed at 2243 cm<sup>–1</sup>, ~110 cm<sup>–1</sup> higher than that in K<sub>2</sub>[Pd(CN)<sub>4</sub>] (2135.8 cm<sup>–1</sup>).

The structures of **4b**·2Me<sub>2</sub>CO, **4c**·2CH<sub>2</sub>Cl<sub>2</sub>, and **5c**·2CH<sub>2</sub>Cl<sub>2</sub> were determined by X-ray diffraction. In all cases the anions are square-planar; the anion of **5c** is shown in Figure 2. The M–C and C–N distances of the B(C<sub>6</sub>F<sub>5</sub>)<sub>3</sub> adducts are remarkably similar to those found in the solid-state structures of K<sub>2</sub>–Ni(CN)<sub>4</sub> and Rb<sub>2</sub>Ni(CN)<sub>4</sub>·H<sub>2</sub>O;<sup>19,20</sup> for example, the average Ni–C distance in **4c** (1.856(2) Å) is essentially identical to that in K<sub>2</sub>Ni(CN)<sub>4</sub> (1.87(3) Å). The C–N bond distances in K<sub>2</sub>Ni(CN)<sub>4</sub> and Rb<sub>2</sub>Ni(CN)<sub>4</sub>·H<sub>2</sub>O are almost identical to those in **4b**, **4c**, and **5c**, (as far as is possible to judge in view of the comparatively large standard deviations in the parent cyano complexes). A comparison of bond distances in cyano complexes is given in Table 2.

**Reactivity Studies.** The solution chemistry of the new activators **1** and **4** in reaction with various metallocenes was studied by NMR spectroscopy.

Some time ago we showed that the reaction of [CPh<sub>3</sub>]-[B(C<sub>6</sub>F<sub>5</sub>)<sub>4</sub>] with L<sub>2</sub>ZrMe<sub>2</sub> (L<sub>2</sub> = Cp<sub>2</sub> or SBI; SBI = *rac*-Me<sub>2</sub>-Si(Ind)<sub>2</sub>) in dichloromethane at –60 °C formed the methyl-

(15) Bosch, B. E.; Erker, G.; Fröhlich, R.; Meyer, O. *Organometallics* **1997**, *16*, 5449.

(16) Adducts of B(C<sub>6</sub>F<sub>5</sub>)<sub>3</sub> with neutral (a–d) and anionic (e–h) oxo and nitrido complexes have recently been described: (a) Galsworthy, J. R.; Green, M. L. H.; Müller, M.; Prout, K. J. *Chem. Soc., Dalton Trans.* **1997**, 1309. (b) Galsworthy, J. R.; Green, J. C.; Green, M. L. H.; Müller, M. J. *Chem. Soc., Dalton Trans.* **1998**, 15. (c) Doerr, L. H.; Galsworthy, J. R.; Green, M. L. H.; Leech, M. A. *J. Chem. Soc., Dalton Trans.* **1998**, 2483. (d) Doerr, L. H.; Galsworthy, J. R.; Green, M. L. H.; Leech, M. A.; Müller, M. J. *Chem. Soc., Dalton Trans.* **1998**, 3191. (e) Doerr, L. H.; Graham, A. J.; Green, M. L. H. *J. Chem. Soc., Dalton Trans.* **1998**, 3941. (f) Barrado, G.; Doerr, L. H.; Green, M. L. H.; Leech, M. A. *J. Chem. Soc., Dalton Trans.* **1999**, 1061. (g) Abram, U.; Kohl, F. J.; Öfele, K.; Herrmann, W. A.; Voigt, A.; Kirmse, R. Z. *Anorg. Allg. Chem.* **1998**, 624, 934. (h) Abram, U. Z. *Anorg. Allg. Chem.* **1999**, 625, 839. See also Scott, R. N.; Shriver, D. F.; Lehman, D. D. *Inorg. Chim. Acta* **1970**, *4*, 73.

(17) Beck, M. T. *Pure Appl. Chem.* **1987**, *59*, 1703.

(18) Kubas, G. J.; Jones, L. H. *Inorg. Chem.* **1974**, *13*, 2816.

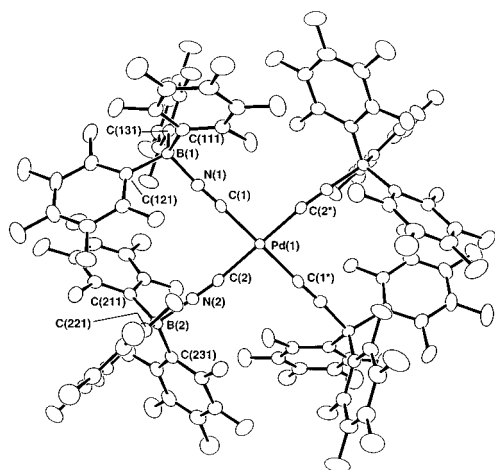
(19) Vanneberg, N. G. *Acta Chem. Scand.* **1964**, *18*, 2385.

(20) Dupont, L. *Acta Crystallogr.* **1970**, *B26*, 964.



**Table 2.** Comparison of Bond Distances in Metal–Cyano Complexes [Å]

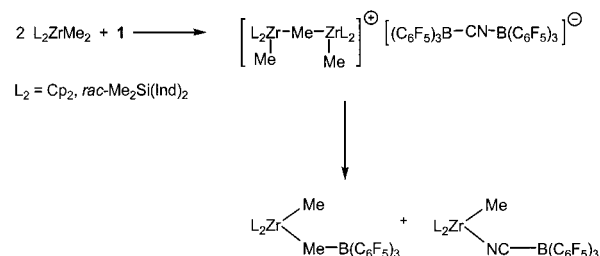
complex	M–C1	M–C2	C1–N1	C2–N2	N1–B1	N2–B2
K <sub>2</sub> [Ni(CN) <sub>4</sub> ]	1.90(3)	1.84(3)	1.15(5)	1.11(5)		
<b>4b</b>	1.851(2)	1.856(2)	1.43(3)	1.143(2)	1.582(3)	1.582(3)
<b>4c</b>	1.855(2)	1.862(2)	1.145(2)	1.146(2)	1.574(2)	1.574(2)
Rb <sub>2</sub> [Pd(CN) <sub>4</sub> ]·H <sub>2</sub> O	1.967(20)	2.038(23)	1.164(26)	1.093(28)		
<b>5c</b>	1.989(2)	1.995(2)	1.126(3)	1.126(3)	1.577(3)	1.571(3)

**Figure 2.** Structure of the [Pd{CNB(C<sub>6</sub>F<sub>5</sub>)<sub>3</sub>}<sub>4</sub>]<sup>2−</sup> anion in **5c**, showing the atomic numbering scheme. Ellipsoids are drawn at 40% probability level.

bridged binuclear cations [(L<sub>2</sub>ZrMe)<sub>2</sub>(μ-Me)]<sup>+</sup>, even in the presence of excess trityl salt.<sup>21</sup> Conversion to the mononuclear species [L<sub>2</sub>ZrMe]<sup>+</sup> occurred only on warming but was accompanied by rapid decomposition in the chlorinated solvent. For comparison with the behavior of activators **1** and **4**, the reactions of L<sub>2</sub>ZrMe<sub>2</sub> with [CPh<sub>3</sub>][B(C<sub>6</sub>F<sub>5</sub>)<sub>4</sub>] were reinvestigated in benzene-*d*<sub>6</sub> at room temperature.

Treatment of [CPh<sub>3</sub>][B(C<sub>6</sub>F<sub>5</sub>)<sub>4</sub>] with an excess of L<sub>2</sub>ZrMe<sub>2</sub> generates the binuclear zirconocene cations [(L<sub>2</sub>ZrMe)<sub>2</sub>(μ-Me)]<sup>+</sup>·[B(C<sub>6</sub>F<sub>5</sub>)<sub>4</sub>]<sup>−</sup> in benzene solution at 298 K. The zirconocene concentration was kept low (0.6 < [Zr]<sub>tot</sub> < 2.5 mmol L<sup>−1</sup>) to prevent the formation of higher aggregates and the precipitation of ionic species as oils. Even in samples with a reactant ratio of 1:1 only the binuclear cations are observed as the initial products. The slow formation of mononuclear cationic zirconocene complexes [L<sub>2</sub>ZrMe<sup>+</sup>···B(C<sub>6</sub>F<sub>5</sub>)<sub>4</sub>]<sup>−</sup> is seen after a few minutes. In the case of L<sub>2</sub> = SBI the kinetics of this transformation were determined. The reaction of [(SBI)ZrMe]<sub>2</sub>(μ-Me)·[B(C<sub>6</sub>F<sub>5</sub>)<sub>4</sub>] with excess [CPh<sub>3</sub>][B(C<sub>6</sub>F<sub>5</sub>)<sub>4</sub>] proceeds cleanly to give the ion pair [(SBI)ZrMe]<sup>+</sup>···B(C<sub>6</sub>F<sub>5</sub>)<sub>4</sub><sup>−</sup> and follows pseudo-first-order kinetics, *k* = 3 × 10<sup>−4</sup> s<sup>−1</sup> (298 K). The mononuclear complex is stable in benzene under these conditions. A comparable slow reaction was observed for the Cp<sub>2</sub>ZrMe<sub>2</sub> system, which forms a far less stable binuclear cation.

The reaction of L<sub>2</sub>ZrMe<sub>2</sub> with **1** in C<sub>6</sub>D<sub>6</sub> proceeds in a similar manner, forming [(L<sub>2</sub>ZrMe)<sub>2</sub>(μ-Me)][CN{B(C<sub>6</sub>F<sub>5</sub>)<sub>3</sub>}<sub>2</sub>] as the initial product at 25 °C (Scheme 2). The binuclear ion pair formed from the Cp<sub>2</sub>ZrMe<sub>2</sub> system, [(Cp<sub>2</sub>ZrMe)<sub>2</sub>(μ-Me)]<sup>+</sup>···(C<sub>6</sub>F<sub>5</sub>)<sub>3</sub>BCNB(C<sub>6</sub>F<sub>5</sub>)<sub>3</sub><sup>−</sup>, proved to be relatively unstable at room temperature. The spectrum shows complete decomposition of a benzene solution with [Zr]<sub>tot</sub> = 2 mmol/L after 5 min. It was

**Scheme 2**

not possible to obtain a clean spectrum without decomposition products. The formation of the zwitterionic B(C<sub>6</sub>F<sub>5</sub>)<sub>3</sub> adduct, Cp<sub>2</sub>ZrMe(μ-Me)B(C<sub>6</sub>F<sub>5</sub>)<sub>3</sub>, and one other species, presumably Cp<sub>2</sub>ZrMe(μ-N≡C)B(C<sub>6</sub>F<sub>5</sub>)<sub>3</sub>, could be detected.

The dimethylsilyl-bridged complex forms a more stable binuclear complex. Decomposition of [(SBI)ZrMe]<sub>2</sub>(μ-Me)·[CN{B(C<sub>6</sub>F<sub>5</sub>)<sub>3</sub>}<sub>2</sub>] occurs within hours; complete decomposition of a sample could be detected after 24 h at 298 K in benzene solution. Two main products are detected: the B(C<sub>6</sub>F<sub>5</sub>)<sub>3</sub> adduct, (SBI)ZrMe(μ-Me)B(C<sub>6</sub>F<sub>5</sub>)<sub>3</sub>, and one other species, assigned to (SBI)ZrMe(μ-N≡C)B(C<sub>6</sub>F<sub>5</sub>)<sub>3</sub>. Mononuclear cation–anion pairs of the type [L<sub>2</sub>ZrMe<sup>+</sup>···(C<sub>6</sub>F<sub>5</sub>)<sub>3</sub>BCNB(C<sub>6</sub>F<sub>5</sub>)<sub>3</sub>]<sup>−</sup> are not observed.

The reactions of Cp<sub>2</sub>ZrMe<sub>2</sub> and (SBI)ZrMe<sub>2</sub> with the nickel complex **4c** again give initially the corresponding binuclear μ-Me cations as the only observable metallocene products. Because of the poor solubility of **4c** in benzene, measurements were initially carried out in CD<sub>2</sub>Cl<sub>2</sub>. The primary product, [(SBI)ZrMe]<sub>2</sub>(μ-Me)<sub>2</sub>[Ni{CNB(C<sub>6</sub>F<sub>5</sub>)<sub>3</sub>}<sub>4</sub>], proved surprisingly stable in the chlorinated solvent at room temperature, although some decomposition was apparent after ~15 min.

For reactions with **4c** in C<sub>6</sub>D<sub>6</sub> the addition of up to 20 vol % 1,2-difluorobenzene was required to achieve adequate solubility. Mixture of **4c** with excess L<sub>2</sub>ZrMe<sub>2</sub> in C<sub>6</sub>D<sub>6</sub>/C<sub>6</sub>H<sub>4</sub>F<sub>2</sub> gave [(L<sub>2</sub>ZrMe)<sub>2</sub>(μ-Me)]<sub>2</sub><sup>+</sup>[Ni{CNB(C<sub>6</sub>F<sub>5</sub>)<sub>3</sub>}<sub>4</sub>]<sup>2−</sup>, as expected (L<sub>2</sub> = Cp<sub>2</sub>, SBI), together with unreacted L<sub>2</sub>ZrMe<sub>2</sub>. These binuclear complexes are more stable than their [CN{B(C<sub>6</sub>F<sub>5</sub>)<sub>3</sub>}<sub>2</sub>]<sup>−</sup> analogues; a sample of [(Cp<sub>2</sub>ZrMe)<sub>2</sub>(μ-Me)]<sub>2</sub>[Ni{CNB(C<sub>6</sub>F<sub>5</sub>)<sub>3</sub>}<sub>4</sub>] decomposed completely only after 60 min, while a sample of [(SBI)ZrMe]<sub>2</sub>(μ-Me)<sub>2</sub>[Ni{CNB(C<sub>6</sub>F<sub>5</sub>)<sub>3</sub>}<sub>4</sub>] showed minor signs of decomposition only after 30 min. In both cases the B(C<sub>6</sub>F<sub>5</sub>)<sub>3</sub> adducts, L<sub>2</sub>ZrMe(μ-Me)B(C<sub>6</sub>F<sub>5</sub>)<sub>3</sub>, were detected as the only decomposition products; there was no evidence for CN-bridged decomposition products, such as L<sub>2</sub>ZrMe(μ-NC)Ni{CNB(C<sub>6</sub>F<sub>5</sub>)<sub>3</sub>}<sub>3</sub>.

A similar sequence of events is observed in the presence of AlMe<sub>3</sub> which is known to form comparatively stable heterobinuclear cations [Cp<sub>2</sub>Zr(μ-Me)<sub>2</sub>AlMe<sub>2</sub>]<sup>+</sup>.<sup>21</sup> For example, a mixture of Cp<sup>''</sup><sub>2</sub>ZrMe<sub>2</sub>, **1**, and AlMe<sub>3</sub> in a 1:1:1.5-ratio forms the heterobinuclear complex [Cp<sup>''</sup><sub>2</sub>Zr(μ-Me)<sub>2</sub>AlMe<sub>2</sub>]<sup>+</sup>[CN{B(C<sub>6</sub>F<sub>5</sub>)<sub>3</sub>}<sub>2</sub>]<sup>−</sup> (Cp<sup>''</sup> = 1,3-C<sub>5</sub>H<sub>3</sub>(SiMe<sub>3</sub>)<sub>2</sub>). The NMR spectrum in C<sub>6</sub>D<sub>6</sub> at room temperature is broad, but the product is unequivocally characterized in CD<sub>2</sub>Cl<sub>2</sub> at −50 °C.

This reaction was repeated on a preparative scale in toluene. Treatment of a mixture of Cp<sup>''</sup><sub>2</sub>ZrMe<sub>2</sub> and excess AlMe<sub>3</sub> with **1** gave an oily precipitate of [Cp<sup>''</sup><sub>2</sub>Zr(μ-Me)<sub>2</sub>AlMe<sub>2</sub>][NC-

(21) (a) Bochmann, M.; Lancaster, S. *J. Angew. Chem., Int. Ed. Engl.* **1994**, *33*, 1634. (b) Bochmann, M.; Lancaster, S. *J. Organomet. Chem.* **1995**, *497*, 55. (c) For related MeB(C<sub>6</sub>F<sub>5</sub>)<sub>3</sub><sup>−</sup> complexes, see: Haselwander, T.; Beck, S.; Brintzinger, H. H. In *Ziegler Catalysts*; Fink, G., Mülhaupt, R., Brintzinger, H. H., Eds.; Springer, Berlin, 1995; p 181. Beck, S.; Prosen, M. H.; Brintzinger, H. H. *J. Mol. Catal. A: Chem.* **1998**, *128*, 41.

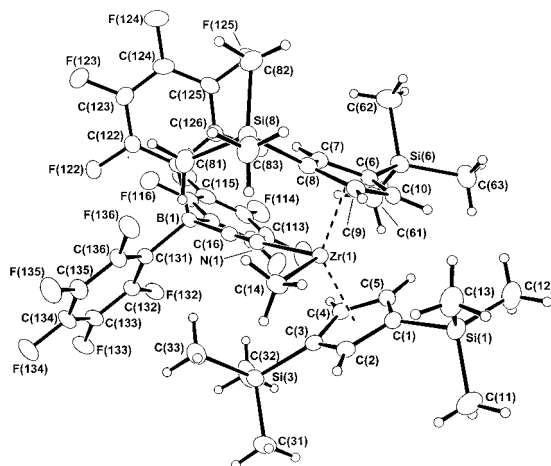
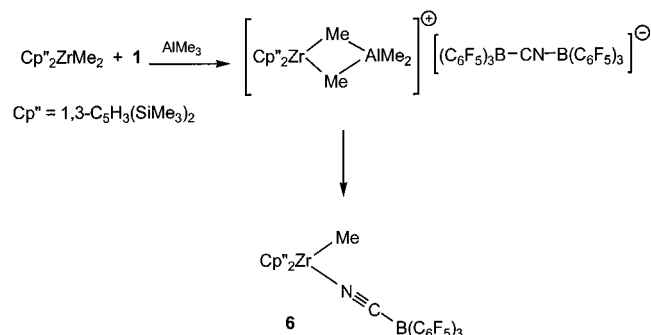


**Figure 3.** Molecular structure of  $\text{Cp}''_2\text{ZrMe}(\mu\text{-NC})\text{B}(\text{C}_6\text{F}_5)_3$  **6**, showing the atomic numbering scheme. Ellipsoids are drawn at 40% probability level.

### Scheme 3



$\{\text{B}(\text{C}_6\text{F}_5)_3\}_2$  (Scheme 3). After this mixture was stirred at room temperature for 30 min, the precipitate dissolved to afford a clear solution from which pale-yellow crystals were isolated. The product was identified as the cyanoborate complex,  $\text{Cp}''_2\text{ZrMe}(\mu\text{-NC})\text{B}(\text{C}_6\text{F}_5)_3$  **6**. The structure of **6**·toluene was confirmed by X-ray crystallography (Figure 3).

The Zr–CH<sub>3</sub> and Zr–N bond lengths of **6** are essentially identical, 2.254(3) and 2.259(2) Å, respectively, and closely comparable to the terminal Zr–CH<sub>3</sub> distance in  $\text{Cp}''_2\text{ZrMe}(\mu\text{-Me})\text{B}(\text{C}_6\text{F}_5)_3$  (2.260(4) Å).<sup>22</sup> The C–N distance of 1.149(3) Å is almost identical to the corresponding value in **1**, while the B–C distance in **6** is slightly longer, 1.614(4) Å compared to 1.583(2) Å. The C(14)–Zr–N(1) angle of 102.60(10)° is marginally wider than the Me–Zr–Me angle in the related complex  $\text{Cp}''_2\text{ZrMe}(\mu\text{-Me})\text{B}(\text{C}_6\text{F}_5)_3$  (97.1(2)°).

On the basis of the X-ray diffraction data alone it is not possible to decide unequivocally whether the CN moiety is N-bound or C-bound to zirconium, although refinement with the thermal parameters for Zr–N gave slightly better results. The anion of **1** shows two <sup>11</sup>B NMR resonances, a broadened signal at  $\delta$  –11.94 for B–N, and a sharp resonance for B–C at  $\delta$  –21.68. Complex **6** only shows a sharp signal at  $\delta$  –19.57, that is, the boron atom is C-bound, and there is no C/N bond isomerization.

**Polymerization Studies and Anion Effects.** As stated in the Introduction, the nature of the counteranion and its coordinating ability can exercise a profound effect on catalyst activity. Thus, even weakly coordinating anions such as  $[\text{MeB}(\text{C}_6\text{F}_5)_3]^-$  and  $[\text{B}(\text{C}_6\text{F}_5)_4]^-$  are involved in dissociation equilibria<sup>2a</sup> with cationic

metallocene species and may form solvated and solvent-separated ion pairs.<sup>23</sup> As Brintzinger et al. showed recently, these ion pairs may associate in low-polarity solvents such as benzene or toluene to give ion quadruplets, at least in the absence of olefin monomer.<sup>24</sup> The importance of ion-pair association has been underlined further by theoretical modeling studies which show the displacement of the counteranion from the metal coordination sphere by ethene as a low-energy pathway that probably constitutes the largest contribution toward the activation barrier of the chain growth process.<sup>25</sup>

Although the expectation of significant anion effects on the rate of polymerization is therefore reasonable, differences between chemically closely related anions in high-activity catalysts can be difficult to assess quantitatively. For example, early studies on the activity and stereoselectivity of zirconocenes as a function of the anions  $[\text{MeB}(\text{C}_6\text{F}_5)_3]^-$ ,  $[\text{PhCH}_2\text{B}(\text{C}_6\text{F}_5)_3]^-$ ,  $[\text{B}(\text{C}_6\text{F}_5)_4]^-$ , and  $[\text{Me-MAO}]^-$  had shown that the effects were readily obscured by differences in reaction exotherms that proved difficult to control.<sup>26</sup> In addition, it is well-known that the activity of a given catalyst system can vary widely with reaction conditions, in particular activator:catalyst ratio, polymerization times, and catalyst concentration.<sup>27</sup> This is perhaps best illustrated by Möhring and Coville's compilation of literature data for the activity of the "standard" ethene polymerization catalyst  $\text{Cp}_2\text{ZrCl}_2/\text{MAO}$ , which cover a range of 4 orders of magnitude.<sup>28</sup> We therefore saw the need to arrive at an experimental protocol that would allow an assessment of anion and ligand effects in a more quantitative fashion.

Preliminary ethene polymerizations were carried out under 1 bar monomer pressure at 60 °C using (SBI)ZrMe<sub>2</sub> in 50 mL of toluene in the presence of 200 μmol  $\text{AlBu}_3$  as scavenger, with a Zr:activator ratio of 1:1 and a stirring rate of 1000 rpm, to develop a standard set of reaction conditions. With both  $[\text{CPh}_3][\text{B}(\text{C}_6\text{F}_5)_4]$  and **1**, high polymerization activities were observed. However, in most reactions activator addition led to the instantaneous formation of a surface polymer film which was bound to impede monomer uptake from the gas phase, and mass-transport limitation was therefore suspected.

This was borne out by the strong *apparent* dependence of catalyst activity on [Zr]. Decreasing [Zr] for a (SBI)ZrMe<sub>2</sub>/  $[\text{CPh}_3][\text{B}(\text{C}_6\text{F}_5)_4]$  catalyst from  $2 \times 10^{-5}$  mol L<sup>–1</sup> to  $4 \times 10^{-6}$  mol L<sup>–1</sup> increased the catalyst productivity figure from  $33.8 \times 10^6$  g PE (mol Zr)<sup>–1</sup> h<sup>–1</sup> bar<sup>–1</sup> to  $168 \times 10^6$  g PE (mol Zr)<sup>–1</sup> h<sup>–1</sup> bar<sup>–1</sup> (Figure 4). However, closer inspection showed that in all reactions almost identical amounts of polymer had been produced, a clear case of mass-transport limitation due to rapid monomer consumption from the solution phase. Evidently chain propagation in these systems is significantly faster than monomer diffusion into the solution, and therefore, *none of these values should be regarded as a true reflection of the actual activity of this catalyst system.*

Reducing the catalyst concentration below  $\sim 4 \times 10^{-6}$  mol L<sup>–1</sup> in an effort to overcome problems of monomer depletion proved problematic since very highly diluted stock solutions

(23) Beck, S.; Prosenc, M. H.; Brintzinger, H. H.; Goretzki, R.; Herfert, N.; Fink, G. *J. Mol. Catal.* **1996**, *111*, 67.

(24) Beck, S.; Geyer, A.; Brintzinger, H. H. *Chem. Commun.* **1999**, 2477.

(25) (a) Chan, M. S. W.; Vanka, K.; Pye, C. C.; Ziegler, T. *Organometallics* **1999**, *18*, 4624. (b) Vanka, V.; Chan, M. S. W.; Pye, C. C.; Ziegler, T. *Organometallics* **2000**, *19*, 1841.

(26) Lancaster, S. J. Ph.D. Thesis, University of East Anglia, 1995.

(27) (a) Kaminsky, W.; Miri, M.; Sinn, H.; Woldt, R. *Macromol. Chem. Rapid Commun.* **1983**, *4*, 417. (b) Janiak, C.; Versteeg, U.; Lange, K. C. H.; Weimann, R.; Hahn, E. *J. Organomet. Chem.* **1995**, *501*, 219. (c) Janiak, C.; Lange, K. C. H.; Versteeg, U.; Lentz, D.; Budzelaar, P. H. M. *Chem. Ber.* **1996**, *129*, 1517.

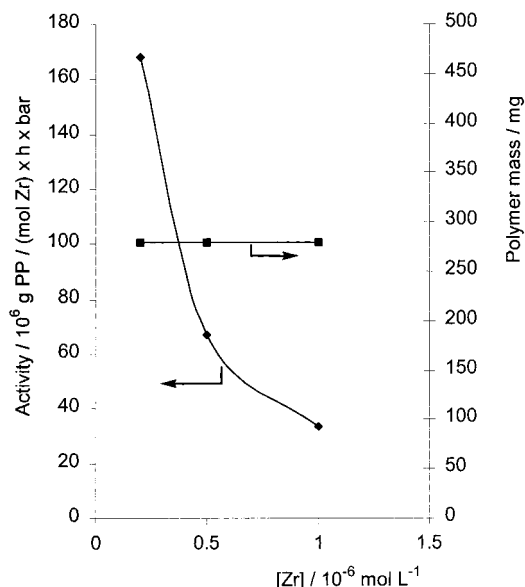
(28) Möhring, P. C.; Coville, N. J. *J. Organomet. Chem.* **1994**, *479*, 1.

(22) Bochmann, M.; Lancaster, S. J.; Hursthouse, M. B.; Malik, K. M. A. *Organometallics* **1994**, *13*, 2235.

**Table 3.** Ethene Polymerizations with Titanium and Zirconium Catalysts as a Function of Anion Structure<sup>a</sup>

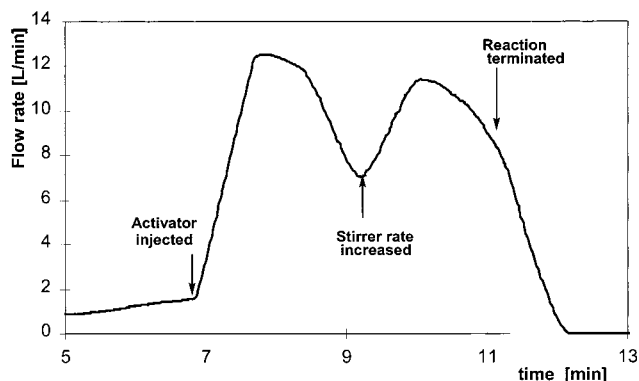
metallocene ( $\mu\text{mol}$ )	activator <sup>b</sup> ( $\mu\text{mol}$ )	AlBu <sub>3</sub> ( $\mu\text{mol}$ )	temp [°C]	time [s]	polymer yield [g]	productivity <sup>c</sup>	$M_w \times 10^{-3}$	$M_w/M_n$	$T_m$ [°C]
(SBI)ZrMe <sub>2</sub> (1.0)	B(C <sub>6</sub> F <sub>5</sub> ) <sub>4</sub> (1.0)	200	60	180	0.68	13.6			n.d.
(SBI)ZrMe <sub>2</sub> (0.2)	B(C <sub>6</sub> F <sub>5</sub> ) <sub>4</sub> (0.2)	200	60	30	0.28	168	195.5	2.7	135.4
(SBI)ZrMe <sub>2</sub> (1.0)	B(C <sub>6</sub> F <sub>5</sub> ) <sub>4</sub> (1.0)	200	60	30	0.28	33.8			135.7
(SBI)ZrMe <sub>2</sub> (0.2)	B(C <sub>6</sub> F <sub>5</sub> ) <sub>4</sub> (0.2)	200	60	10	0.21	450	178	2.7	n.d.
(SBI)ZrMe <sub>2</sub> (1.0)	B(C <sub>6</sub> F <sub>5</sub> ) <sub>3</sub> (1.0)	200	60	180	0.70	14.0	225.5	3.0	n.d.
(SBI)ZrMe <sub>2</sub> (0.5)	B(C <sub>6</sub> F <sub>5</sub> ) <sub>3</sub> (0.5)	200	60	30	0.29	69.6			137.3
CGCTiBz <sub>2</sub> (0.2)	<b>1</b> (0.2)	100	60	30	0.21	126			
CGCTiBz <sub>2</sub> (0.5)	<b>1</b> (0.5)	100	60	30	0.26	62.4			
CGCTiBz <sub>2</sub> (1.0)	<b>1</b> (1.0)	100	60	30	0.37	44.4	304	3.0	136.9
CGCTiBz <sub>2</sub> (1.0)	B(C <sub>6</sub> F <sub>5</sub> ) <sub>4</sub> (1.0)	100	60	30	0.30	36	254	3.3	137.3
CGCTiBz <sub>2</sub> (1.0)	B(C <sub>6</sub> F <sub>5</sub> ) <sub>3</sub> (1.0)	100	60	30	0.20	24			138.1

<sup>a</sup> Conditions: 1 bar ethene pressure, 50 mL toluene, stirring rate 1000 rpm. <sup>b</sup> B(C<sub>6</sub>F<sub>5</sub>)<sub>4</sub> = [CPh<sub>3</sub>][B(C<sub>6</sub>F<sub>5</sub>)<sub>4</sub>]. <sup>c</sup> In 10<sup>6</sup> g PE/(mol M)·h·bar.

**Figure 4.** Dependence of catalyst activity and polymer yield in ethene polymerizations with (SBI)ZrMe<sub>2</sub>/[CPh<sub>3</sub>][B(C<sub>6</sub>F<sub>5</sub>)<sub>4</sub>]/AlBu<sub>3</sub> (60 °C, 1 bar, 30 s), an illustration of mass-transport limitation.

of zirconocene dimethyls are very prone to hydrolysis and tend to give poorly reproducible results. Ethene polymerizations were therefore conducted in a 5 L autoclave under 7 bar ethene. This allowed the maximum concentration of active cationic zirconium species to be reduced to  $6.7 \times 10^{-8} \text{ mol L}^{-1}$ . With (SBI)ZrMe<sub>2</sub>/1/AlBu<sub>3</sub> (5:1:1000) at a start temperature of 60 °C very rapid polymerization was observed, accompanied by a temperature increase of ~40 °C.<sup>29</sup> It proved difficult to pump in feed gas sufficiently fast to maintain the reactor pressure which dropped within 1 min from 7 to 2 bar. The gas flow diagram (Figure 5) shows that even under these conditions the reaction is still diffusion limited, that is, the gas flow is very sensitive to the stirrer speed. After 4 min the reactor was filled with swollen polymer, and the reaction was terminated. The lower limit estimate of catalyst productivity under these conditions was  $7.6 \times 10^8 \text{ g PE (mol Zr)}^{-1} \text{ h}^{-1} \text{ bar}^{-1}$ . Assuming 100% participation of all cationic zirconocene centers in chain growth, this productivity corresponds to a monomer insertion rate of over  $5 \times 10^4 \text{ s}^{-1}$  averaged over the 4 min period. Initial insertion rates are presumably much higher. Neither in these autoclave reactions nor in reactions at 1 bar at lower temperatures were we able to demonstrate the absence of mass-transport limitations in the case of ethene polymerizations.

(29) The power output of 1  $\mu\text{mol}$  catalyst under these conditions is about 4 kW. Internal cooling of the autoclave was not attempted.

**Figure 5.** Gas-flow profile of an ethene polymerization with (SBI)-ZrMe<sub>2</sub>/1/AlBu<sub>3</sub> under pressure (5  $\mu\text{mol}$  Zr, 1  $\mu\text{mol}$  **1**, 1 mmol Al; 60 °C, initial pressure 7 bar, 3 L toluene), showing (a) injection of the activator; (b) increase of stirrer speed from 500 to 800 rpm; (c) termination by methanol injection. After 2 min, gas uptake was impeded by large amounts of swollen polymer.

Even in ethene polymerizations at 1 bar noticeable reaction exotherms were observed, and for this reason comparable but less active catalysts were sought. Earlier work on anion effects by Marks et al. had suggested that titanium catalysts of the “constrained geometry” type, such as Me<sub>2</sub>Si(C<sub>5</sub>Me<sub>4</sub>)(NBu<sup>t</sup>)TiR<sub>2</sub> (CGCTiR<sub>2</sub>), gave ethene polymerization activities that were up to 2 orders of magnitude lower than those of zirconocenes, for example,  $0.08$  and  $1.56 \times 10^6 \text{ g PE (mol Ti)}^{-1} \text{ h}^{-1} \text{ bar}^{-1}$  for [CGCTiMe][MeB(C<sub>6</sub>F<sub>5</sub>)<sub>3</sub>] and [CGC<sup>H</sup>Ti][B(C<sub>6</sub>F<sub>5</sub>)<sub>4</sub>], respectively.<sup>7d,f</sup> We therefore decided to compare our zirconocene results with the system CGCTiR<sub>2</sub>/activator/AlBu<sub>3</sub>.

Ethene polymerizations with (SBI)ZrMe<sub>2</sub> and CGCTiBz<sub>2</sub> activated with **1**, and for comparison, [CPh<sub>3</sub>][B(C<sub>6</sub>F<sub>5</sub>)<sub>4</sub>] and B(C<sub>6</sub>F<sub>5</sub>)<sub>3</sub> are collected in Table 3. In our hands the titanium catalysts exhibited activities comparable to those of zirconocenes and were 10–100 times more active than previously reported. In part this difference may be due to the presence of the AlBu<sub>3</sub> scavenger in our system.<sup>30</sup> All three activators produced catalysts of broadly comparable activities which decreased in the order [CN(B(C<sub>6</sub>F<sub>5</sub>)<sub>3</sub>)<sub>2</sub>]<sup>−</sup> ≥ [B(C<sub>6</sub>F<sub>5</sub>)<sub>4</sub>]<sup>−</sup> > B(C<sub>6</sub>F<sub>5</sub>)<sub>3</sub>. In the titanium system, too, strictly isothermal conditions proved difficult to establish.

Propene polymerizations present a different scenario. Some time ago we reported that Cp<sup>\*</sup>TiMe<sub>3</sub>/B(C<sub>6</sub>F<sub>5</sub>)<sub>3</sub> polymerizes propene to a very high molecular weight elastomeric polymer with narrow polydispersity.<sup>31</sup> In this system the polymer yield

(30) AlBu<sub>3</sub> can also act as an alkylating agent, although the extent of this reaction depends on the transition-metal alkyl. With (SBI)ZrMe<sub>2</sub> and CGCTiMe<sub>2</sub> in the presence of excess AlBu<sub>3</sub>, rapid Me/*i*-Bu exchange is observed, while CGCTi(CH<sub>2</sub>Ph)<sub>2</sub> remains essentially unreacted after 5 h at 25 °C (Al:Ti = 8:1, C<sub>6</sub>D<sub>6</sub>).



**Table 4.** Propene Polymerizations with Titanium and Zirconium Methyl Complexes as a Function of Anion Structure<sup>a</sup>

entry no.	metallocene ( $\mu\text{mol}$ )	activator <sup>b</sup> ( $\mu\text{mol}$ )	AlBu <sub>3</sub> [ $\mu\text{mol}$ ]	toluene [mL]	start temp [°C]	time [min]	$\Delta T^c$ [°C]	polymer yield [g]	productivity <sup>d</sup>	$M_w \times 10^{-3}$	$M_w/M_n$	$T_m$ [°C]
1	(SBI)ZrMe <sub>2</sub> (0.5)	<b>1</b> (0.5)	100	100	0	0.5	4	0.89	167.1			154.4
2	(SBI)ZrMe <sub>2</sub> (0.5)	<b>1</b> (0.5)	100	100	20	0.5	6	0.88	297.5	109	1.9	150.5
3	(SBI)ZrMe <sub>2</sub> (1.0)	<b>1</b> (1.0)	100	100	20	0.5	14	1.64	277.2	95	2.0	
4	(SBI)ZrMe <sub>2</sub> (1.0)	<b>1</b> (1.0)	100	100	20	1.0	6	0.95	160.6			
5	(SBI)ZrMe <sub>2</sub> (1.0)	<b>1</b> (1.0)	100	1000	20	1.0	0	0.89	150.4	105	3.8	
6	(SBI)ZrMe <sub>2</sub> (0.5)	B(C <sub>6</sub> F <sub>5</sub> ) <sub>4</sub> <sup>-</sup> (0.5)	100	100	20	0.5	4	0.56	189.3	112	1.9	135.4
7	(SBI)ZrMe <sub>2</sub> (0.5)	B(C <sub>6</sub> F <sub>5</sub> ) <sub>4</sub> <sup>-</sup> (0.5)	100	100	20	1.0	4	0.70	118.3	86.2	2.2	
8	(SBI)ZrMe <sub>2</sub> (0.5)	B(C <sub>6</sub> F <sub>5</sub> ) <sub>4</sub> <sup>-</sup> (0.5)	100	1000	20	1.0	0	0.58	98.0			135.4
9	(SBI)ZrMe <sub>2</sub> (0.5)	B(C <sub>6</sub> F <sub>5</sub> ) <sub>3</sub> (0.5)	100	100	20	10	0	0	0			
10	(SBI)ZrMe <sub>2</sub> (1.0)	B(C <sub>6</sub> F <sub>5</sub> ) <sub>3</sub> (1.0)	100	100	20	10	0	0.19	1.60			
11	(SBI)ZrMe <sub>2</sub> (4.0)	B(C <sub>6</sub> F <sub>5</sub> ) <sub>3</sub> (4.0)	100	100	20	3	1.5	0.20	1.41			146.0
12	(SBI)ZrMe <sub>2</sub> (4.0)	B(C <sub>6</sub> F <sub>5</sub> ) <sub>3</sub> (4.0)	100	100	20	30	6.5	5.35	3.77	67	2.4	144.3
13	(SBI)ZrMe <sub>2</sub> (4.0)	B(C <sub>6</sub> F <sub>5</sub> ) <sub>3</sub> (4.0)	5	100	20	10	0	0.08	0.17			
14	CGCTiMe <sub>2</sub> (0.5)	<b>1</b> (0.5)	100	100	20	0.5	5.5	1.16	392.1	925	3.9	<i>e</i>
15	CGCTiMe <sub>2</sub> (0.5)	<b>1</b> (0.5)	100	100	20	1.0	6.0	1.32	223.1			
16	CGCTiMe <sub>2</sub> (0.5)	<b>1</b> (0.5)	100	1000	20	1.0	0	1.29	218.0	1150	3.7	
17	CGCTiMe <sub>2</sub> (0.5)	B(C <sub>6</sub> F <sub>5</sub> ) <sub>4</sub> <sup>-</sup> (0.5)	100	100	20	0.5	4.5	0.66	223.1			
18	CGCTiMe <sub>2</sub> (0.5)	B(C <sub>6</sub> F <sub>5</sub> ) <sub>4</sub> <sup>-</sup> (0.5)	100	1000	20	1.0	0	1.35	228.2	1640	4.5	
19	CGCTiMe <sub>2</sub> (10.0)	B(C <sub>6</sub> F <sub>5</sub> ) <sub>3</sub> (10.0)	100	100	20	17	0	0.25	1.24			
20	CGCTiMe <sub>2</sub> (25.0)	B(C <sub>6</sub> F <sub>5</sub> ) <sub>3</sub> (25.0)	100	100	20	30	0	1.43	1.60	142	2.4	
21	(SBI)ZrMe <sub>2</sub> (0.5)	<b>4c</b> (0.25) <sup>f</sup>	100	100	20	0.5	2	0.235	56.4	98	2.5	
22	(SBI)ZrMe <sub>2</sub> (1.0)	<b>4c</b> (0.5) <sup>g</sup>	100	100	20	1.0	0	0.787	47.2			
23	(SBI)ZrMe <sub>2</sub> (1.0)	<b>5c</b> (0.5) <sup>g</sup>	100	100	20	1.0	0	0.228	13.7			

<sup>a</sup> Conditions: 1 bar propene pressure, stirring rate 1000 rpm. <sup>b</sup> B(C<sub>6</sub>F<sub>5</sub>)<sub>4</sub> = [CPh<sub>3</sub>][B(C<sub>6</sub>F<sub>5</sub>)<sub>4</sub>]. <sup>c</sup> Internal temperature rise at the end of the run. <sup>d</sup> In 10<sup>6</sup> g PP/(mol M)·[C<sub>3</sub>H<sub>6</sub>]<sup>-1</sup>·h·bar. <sup>e</sup> a-PP, [mm] = 11.0, [mr] = 49.6, [rr] = 39.4%. <sup>f</sup> In 0.25 mL of toluene/1,2-difluorobenzene (75:25). <sup>g</sup> In 0.5 mL of toluene/1,2-difluorobenzene (75:25).

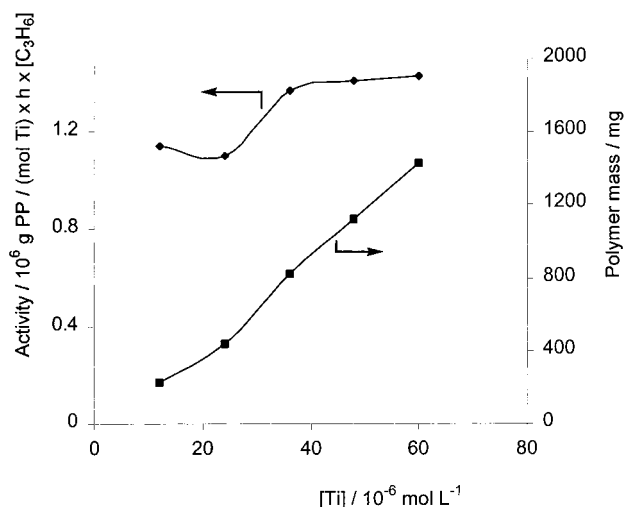


**Figure 6.** Propene polymerization with Cp\*TiMe<sub>3</sub>/B(C<sub>6</sub>F<sub>5</sub>)<sub>3</sub> (20 °C, toluene, 1 bar). The linear increase of polymer yield with [Ti] together with an approximately constant catalyst activity indicates absence of mass-transport limitation.

increased linearly with [Ti], while the productivity values remained approximately constant (Figure 6). These parameters establish that, in contrast to the ethene polymerizations mentioned above, mass-transport limitation is absent, an essential precondition if catalyst productivities are to be related to variables such as ligand structure and the nature of the anion. In the following such a regime was adopted for the assessment of anion effects. To be able to separate the influence of anion structure from other effects on catalyst activity, such as heterogenization of the reaction mixture, catalyst entrapment, increases in solution viscosity, monomer depletion of the reaction medium, and irreversible catalyst deactivation, short and strictly standardized reaction times were employed as far as possible (typically 30 s).

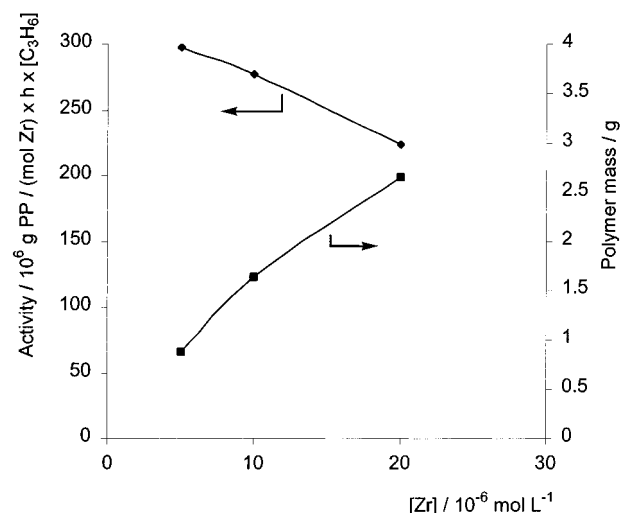


**Figure 7.** Propene polymerizations with (SBI)ZrMe<sub>2</sub>/1/AlBu<sub>3</sub>: dependence of polymer mass and productivity on [Zr] (1 bar, 20 °C, toluene). For experimental details see Table 4.

Polymerizations were carried out at 20 °C in flame-dried glass reactors in 100 mL of toluene and terminated typically after 30 s by methanol injection (Table 4). For the system (SBI)ZrMe<sub>2</sub>/1/AlBu<sub>3</sub> a plot of catalyst productivity as a function of zirconium concentration shows the desired near-linear increase of polymer yield with [Zr] over the chosen range of [Zr] = 5–20 × 10<sup>-6</sup> mol L<sup>-1</sup> (Figure 7). The polymer mass graph shows slight deviation from linearity, and there is some decrease of productivity with increasing [Zr]. We ascribe this effect primarily to the onset of system heterogenization as the product, isotactic polypropene, begins to precipitate. A similar diagram for CGCTiMe<sub>2</sub>/1/AlBu<sub>3</sub> indicates that absence of mass-transport limitation can be assumed up to [Ti] ≤ 2.5 × 10<sup>-5</sup> mol L<sup>-1</sup> (Figure 8).

With (SBI)ZrMe<sub>2</sub>/1/AlBu<sub>3</sub> and [Zr] = 5 × 10<sup>-6</sup> mol L<sup>-1</sup>, productivities were of the order of ~2.8–3.0 × 10<sup>8</sup> g PP (mol Zr)<sup>-1</sup> h<sup>-1</sup> [C<sub>3</sub>H<sub>6</sub>]<sup>-1</sup> (Table 4, entries 2–3). Throughout, the



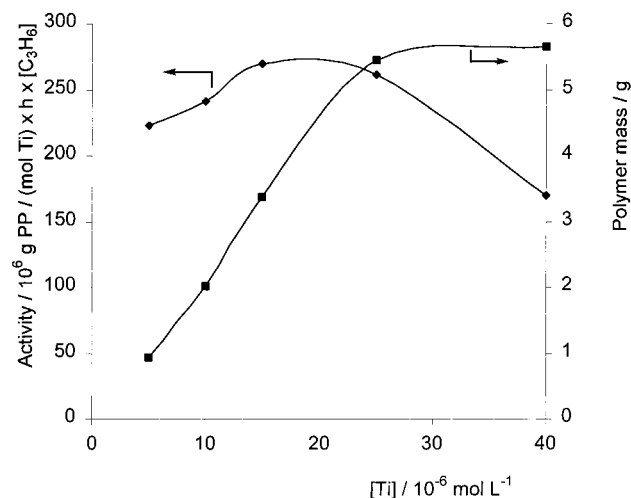


**Figure 8.** Propene polymerizations with CGCTiMe<sub>2</sub>/1/AlBu<sub>3</sub>: dependence of polymer mass and productivity on [Ti] (1 bar, 0 °C, toluene).

productivities obtained with activator **1** were about 1.3–1.5 times higher than with [B(C<sub>6</sub>F<sub>5</sub>)<sub>4</sub>]<sup>−</sup> as counteranion. As was seen in ethene polymerizations, the titanium system CGCTiMe<sub>2</sub>/1/AlBu<sub>3</sub> gave very similar activities to the zirconocene catalyst (Table 4, entries 14–18). For isolated [CGC<sup>−H</sup>Ti][B(C<sub>6</sub>F<sub>5</sub>)<sub>4</sub>] a propene polymerization productivity of  $2.12 \times 10^6$  g PP (mol Ti)<sup>−1</sup> h<sup>−1</sup> bar<sup>−1</sup> has been reported, although the higher catalyst concentration ([Ti] =  $3 \times 10^{-4}$  mol L<sup>−1</sup>) and the longer reaction time employed in this case (5 min) make a direct comparison difficult.<sup>7d</sup>

With both **1** and [CPh<sub>3</sub>][B(C<sub>6</sub>F<sub>5</sub>)<sub>4</sub>] as activators, the reactions conducted in 100 mL of toluene showed a rise of the internal reactor temperature of 4–6 °C, that is, on this scale and at these catalyst concentrations the reactions could not be kept strictly isothermal. The influence of this temperature effect on activity was probed in some cases by increasing the solvent volume to 1000 mL. To keep activator mixing and quenching times short compared to the duration of the polymerization, the reaction times were extended to 1 min; for comparison, reactions of 1 min duration on a 100 mL scale are also reported. Reducing the catalyst concentration in this way by a factor of 10 did indeed eliminate the reaction exotherm, cf. Table 4, entries 4/5, 7/8, and 15/16. At the same time, the closely comparable activity figures for these runs are a further confirmation that mass-transport effects were absent even in the smaller-scale reactions.

The activation of either (SBI)ZrMe<sub>2</sub> or CGCTiMe<sub>2</sub> with B(C<sub>6</sub>F<sub>5</sub>)<sub>3</sub>/AlBu<sub>3</sub> produces catalysts which are significantly less active, so that strictly comparable reaction conditions could not be maintained. To obtain isolable amounts of polymer, it proved necessary to extend the reaction times to up to 30 min and to increase the catalyst concentration. The productivities were about 2 orders of magnitude below those obtained with the CPh<sub>3</sub><sup>+</sup> salts. Here, too, the titanium and zirconium catalysts gave closely similar results.

There was the possibility that the low activity values might be caused by the destruction of B(C<sub>6</sub>F<sub>5</sub>)<sub>3</sub>, which is known to be able to react with AlR<sub>3</sub> under alkyl exchange and formation of potentially deactivating Al–C<sub>6</sub>F<sub>5</sub> species.<sup>32</sup> This was tested by reducing the Al:Zr ratio from 100:1 to 5:1 (Table 4, entry

13). This, however, led to a further significant reduction in polymer yield, and it appears, therefore, that the observed data are primarily a reflection of the comparatively strong coordinating power of [MeB(C<sub>6</sub>F<sub>5</sub>)<sub>3</sub>]<sup>−</sup>.

In the case of zirconocene catalysts the polymer molecular weights are little influenced by the counteranion. By contrast, CGCTiMe<sub>2</sub> catalysts activated with CPh<sub>3</sub><sup>+</sup> salts give atactic PP with molecular weights ~10 times higher than with B(C<sub>6</sub>F<sub>5</sub>)<sub>3</sub> activation (cf. Table 4, entries 14–18 and 20). With these relatively open catalysts anion coordination evidently assists chain termination.

**Dianions as Counteranions.** For the dianions [M{CNB(C<sub>6</sub>F<sub>5</sub>)<sub>3</sub>}]<sub>2</sub><sup>2−</sup> (M = Ni, Pd) stronger ion–ion interactions and comparatively reduced catalyst activities could be expected. This is no doubt reflected in the comparatively poor solubility of the 2:1 electrolytes [CPh<sub>3</sub>]<sub>2</sub>[M{CNB(C<sub>6</sub>F<sub>5</sub>)<sub>3</sub>}]<sub>2</sub> in neat toluene at room temperature. These compounds do, however, form homogeneous solutions on addition of 25 vol % of 1,2-difluorobenzene; stock solutions of **4c** and **5c** were therefore prepared in toluene/difluorobenzene mixtures. Under these conditions, activation of (SBI)ZrMe<sub>2</sub> with **4c** led to rapid propene polymerization, with activities of up to  $5.6 \times 10^7$  g PP (mol Zr)<sup>−1</sup> h<sup>−1</sup> [C<sub>3</sub>H<sub>6</sub>]<sup>−1</sup> (Table 4, entries 21–23). Although somewhat lower, these values are comparable with those for [CPh<sub>3</sub>][B(C<sub>6</sub>F<sub>5</sub>)<sub>4</sub>] and, once again, are significantly higher than those obtained with the rather slow B(C<sub>6</sub>F<sub>5</sub>)<sub>3</sub>-based system.<sup>33</sup>

**Chloride-Containing Systems.** Some time ago Chien et al. introduced the system Cp<sub>2</sub>ZrCl<sub>2</sub>/AlR<sub>3</sub>/[CPh<sub>3</sub>][B(C<sub>6</sub>F<sub>5</sub>)<sub>4</sub>] as an alternative to the use of preformed metallocene dialkyls as catalyst precursors.<sup>34</sup> In view of the greater stability of highly diluted stock solutions of metallocene dichlorides, compared to dialkyls, this system was briefly examined for comparison (Table 5). Reactions of (SBI)ZrCl<sub>2</sub>/AlBu<sub>3</sub> with **1** gave comparable activities to those shown in Table 4, although the data were less reproducible. The source of these errors was traced to the pre-alkylation time: the activities of the chloride-containing system depend markedly on the time the metal dichloride is allowed to react with AlBu<sub>3</sub>. While the alkylation of zirconocene dichlorides by AlR<sub>3</sub> is fast,<sup>35</sup> in the case of CGCTiCl<sub>2</sub> maximum activity is only reached after a pre-reaction time of 30 min (Figure 9).

## Discussion

The formation of adducts between B(C<sub>6</sub>F<sub>5</sub>)<sub>3</sub> and strongly coordinating anions X<sup>n−</sup>, for example X<sup>n−</sup> = CN<sup>−</sup> or [M(CN)<sub>4</sub>]<sup>2−</sup> (M = Ni, Pd), provides a facile general route for the synthesis of new bulky anions [X{B(C<sub>6</sub>F<sub>5</sub>)<sub>3</sub>}]<sup>n−</sup> in which the negative charge is delocalized and less than unity per boron center. The compounds form stable NHMe<sub>2</sub>Ph<sup>+</sup> and CPh<sub>3</sub><sup>+</sup> salts and are suitable as counteranions in metallocene-based polymerization catalysts.

The reaction of zirconocene dimethyls with **1**, **4c**, or **5c** gives salts of the binuclear cations, [(L<sub>2</sub>ZrMe)<sub>2</sub>(μ-Me)]<sup>+</sup> (L<sub>2</sub> = Cp<sub>2</sub> or SBI), stabilized by the very bulky anions. Although the anions are stable toward electrophiles such as CPh<sub>3</sub><sup>+</sup> in solution and in the solid for indefinite periods, they react slowly with [(L<sub>2</sub>ZrMe)<sub>2</sub>(μ-Me)]<sup>+</sup> to give, predominantly, L<sub>2</sub>ZrMe(μ-Me)B(C<sub>6</sub>F<sub>5</sub>)<sub>3</sub> and L<sub>2</sub>ZrMe(μ-NC)B(C<sub>6</sub>F<sub>5</sub>)<sub>3</sub>. At 20 °C the disappearance

(33) The presence of low concentrations of C<sub>6</sub>H<sub>4</sub>F<sub>2</sub> (0.1–0.25 mL/100 mL toluene) has no effect on catalytic activity.

(34) (a) Chien, J. C. W.; Xu, B. *Makromol. Chem., Rapid Commun.* **1993**, *14*, 109. (b) Chien, J. C. W.; Tsai, W. M. *Makromol. Chem., Macromol. Symp.* **1993**, *66*, 141. (c) Chen, Y. X.; Rausch, M. D.; Chien, J. C. W. *Organometallics* **1994**, *13*, 748.

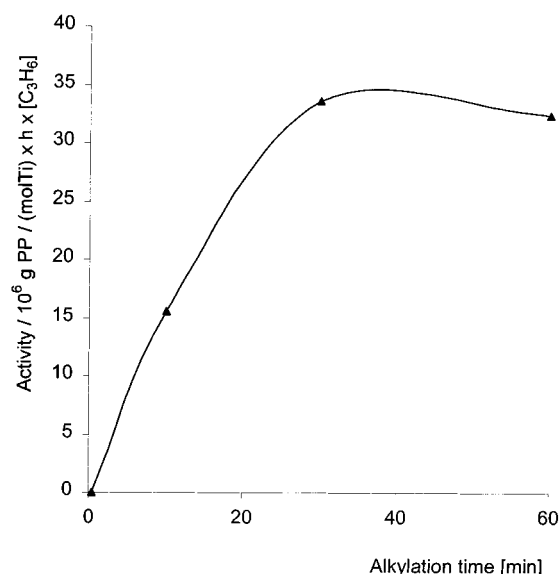
(35) Beck, S.; Brintzinger, H. H. *Inorg. Chim. Acta* **1998**, *270*, 376.

(32) (a) Bochmann, M.; Sarsfield, M. J. *Organometallics* **1998**, *17*, 5908. (b) Lee, C. H.; Lee, S. J.; Park, J. W.; Kim, K. H.; Lee, B. Y.; Oh, J. S. *J. Mol. Catal. A: Chem.* **1998**, *132*, 231. (c) Biagrini, P.; Lugli, G.; Abis, L.; Andreussi, P. (Enichem Elastomeri S.r.l.). Eur. Pat. Appl. EP 0 694 548, 1996.

**Table 5.** Propene Polymerizations with Titanium and Zirconium Dichlorides<sup>a</sup>

entry no.	metallocene ( $\mu\text{mol}$ )	activator <sup>b</sup> ( $\mu\text{mol}$ )	AlBu <sub>3</sub> [ $\mu\text{mol}$ ]	toluene [mL]	start temp [°C]	time [min]	$\Delta T^c$ [°C]	polymer yield [g]	productivity <sup>d</sup>	$T_m$ [°C]
1	(SBI)ZrCl <sub>2</sub> (0.5)	<b>1</b> (0.5)	100	100	20	0.5	6	0.86	290.7	150.4
2	(SBI)ZrCl <sub>2</sub> (1.0)	<b>1</b> (1.0)	100	100	20	0.5	8	1.54	260.3	
3	(SBI)ZrCl <sub>2</sub> (1.0)	B(C <sub>6</sub> F <sub>5</sub> ) <sub>4</sub> <sup>-</sup> (1.0)	100	100	20	1.0	4	0.61	51.4	
4	(SBI)ZrCl <sub>2</sub> (1.0)	B(C <sub>6</sub> F <sub>5</sub> ) <sub>4</sub> <sup>-</sup> (1.0)	100	1000	20	1.0	0	0.63	53.2	
5	(SBI)ZrCl <sub>2</sub> (1.0)	B(C <sub>6</sub> F <sub>5</sub> ) <sub>3</sub> (1.0)	100	100	20	10	0	trace		
6	(SBI)ZrCl <sub>2</sub> (4.0)	B(C <sub>6</sub> F <sub>5</sub> ) <sub>3</sub> (4.0)	100	100	20	30	0	4.48	3.15	146.4
7	CGCTiCl <sub>2</sub> (2.0)	<b>1</b> (2.0)	100 <sup>e</sup>	100	20	0.5	0	0	0	
8	CGCTiCl <sub>2</sub> (2.0)	<b>1</b> (2.0)	100 <sup>f</sup>	100	20	0.5	n.d.	0.56	47.3	

<sup>a</sup> Conditions: 1 bar propene pressure, stirring rate 1000 rpm. <sup>b</sup> B(C<sub>6</sub>F<sub>5</sub>)<sub>4</sub> = [CPh<sub>3</sub>][B(C<sub>6</sub>F<sub>5</sub>)<sub>4</sub>]. <sup>c</sup> Internal temperature rise at the end of the run. <sup>d</sup> In 10<sup>6</sup> g PP/(mol M)·[C<sub>3</sub>H<sub>6</sub>]·h·bar. <sup>e</sup> Alkylation time 0.5 min. <sup>f</sup> Alkylation time 30 min.

**Figure 9.** Propene polymerization activity of CGCTiCl<sub>2</sub>/1/AlBu<sub>3</sub>: dependence of catalyst productivity on pre-alkylation time. Conditions: 2  $\mu\text{mol}$  Ti, Ti:1:Al = 1:1:50, 100 mL toluene, 1 bar, 20 °C.

of [(Cp<sub>2</sub>ZrMe)<sub>2</sub>( $\mu$ -Me)]<sup>+</sup> is complete after 5 min, giving an estimated rate of decomposition of  $\sim 0.003\text{ s}^{-1}$ , while the decomposition of the bulkier SBI analogue requires several hours. From the selective formation of the Zr–NC–B product **6** rather than the Zr–CN–B isomer we conclude that decomposition is initiated by B–N bond dissociation of [CN{B(C<sub>6</sub>F<sub>5</sub>)<sub>3</sub>}<sub>2</sub>]<sup>-</sup>.

The main purpose of this study was the quantification of anion effects on the catalytic activity in olefin polymerization systems with anions of closely similar structures.

Throughout, a catalyst system based on mixtures of a metallocene and activator **1** in the presence of AlBu<sub>3</sub> was used, with an Al:Zr ratio of 200:1 for reactions in 100 mL of toluene, and 2000:1 for reactions on a 1000 mL scale. In our hands the addition of AlBu<sub>3</sub> allowed us to use lower catalyst concentrations without sacrificing reproducibility. Catalyst productivities of repeat reactions were typically reproducible within  $\pm 10\%$  and in many cases 5% or lower. Apart from acting as a scavenger, the metallocene reacts with AlBu<sub>3</sub> under alkyl exchange to give Zr–Bu<sup>i</sup> species. This is beneficial for two reasons: unlike metal–methyl complexes, these isobutyl species are sterically too hindered to form catalytically dormant AlR<sub>3</sub> adducts of the type [L<sub>2</sub>M( $\mu$ -R)<sub>2</sub>AlR<sub>2</sub>]<sup>+</sup>, and second, as Fink has shown,<sup>36</sup> the rate of monomer insertion into a higher M–alkyl

bond can be about 10<sup>2</sup> times faster than insertion into a M–CH<sub>3</sub> bond. These effects serve to maximize the concentration of active species available for the initiation of the chain growth process. The fact that we see consistently higher activities with the (SBI)ZrMe<sub>2</sub> and the CGCTiMe<sub>2</sub> systems than those measured previously<sup>7d,f</sup> is most likely due to generation of higher concentrations of active species in our system.

Catalysts based on (SBI)ZrMe<sub>2</sub>/1/AlBu<sub>3</sub> proved to be very highly active for ethene polymerizations. There was a significant increase in productivity on increasing the ethene pressure up to 7 bar. Although productivities of up to  $7.6 \times 10^8\text{ g PE (mol Zr)}^{-1}\text{ bar}^{-1}\text{ h}^{-1}$  appear to be the highest yet reported, there was evidence that even at the lowest catalyst concentrations we were able to handle reproducibly, catalyst productivity was severely limited by monomer depletion in the solution phase, that is, the data are subject to mass-transport limitations. There is no doubt that this activity figure is far from the upper limit for this catalyst system, and much higher ethene insertion rates than the  $5 \times 10^4\text{ s}^{-1}$  quoted here should be possible with a more appropriate reactor design.

The findings have wider implications. There is much emphasis on the design of new ligands for ethene polymerization catalysts, and activity values are often directly related to ligand structure.<sup>37</sup> However, the productivity of polymerization catalysts is a function of many variables, of which the nature of the ligand may not be the most important. Several scenarios are possible: (a) A catalyst may have an intrinsically high propagation rate  $k_p$  but the productivity is low because the activation method is inefficient and only generates very low concentrations of active species [C\*]. (b) The activation is efficient but the equilibrium between active and dormant species is unfavorable (e.g. because of tight cation–anion interaction, solvent coordination, etc.). (c) Catalyst activation is efficient and [C\*] is high, but a facile decomposition pathway leads to early catalyst deactivation. (d) The catalyst may form high [C\*] and give intrinsically high  $k_p$ , but the monomer concentration is insufficient over the duration of the experiment, or the delivery of monomer to the active center is too slow (i.e., mass-transport limitation). (e) As for (d), but the polymer is poorly soluble, begins to precipitate during the early stages of the reaction, and thereby removes catalyst from the reaction. (f) Activation is efficient, the polymerization is not mass-transport limited, and catalyst productivity is a function of the ligand employed.

It is clear that although most catalytic experiments tend to assume that situation (f) prevails, this is in fact rarely achieved. The results shown here confirm that variations in the mode of catalyst activation and in monomer concentration can produce differences in catalyst activities which are at least as important as changes in ligand structure. Mindful of these difficulties,

(36) (a) Fink, G.; Zoller, W. *Makromol. Chem.* **1981**, 182, 3265. (b) Fink, G.; Schnell, D. *Angew. Makromol. Chem.* **1982**, 105, 31. (c) Mynott, R.; Fink, G.; Fenzl, W. *Angew. Makromol. Chem.* **1987**, 154, 1. (d) Fink, G.; Fenzl, W.; Mynott, R. *Z. Naturforsch., B: Chem. Sci.* **1985**, 40b, 158.

(37) See, for example: Alt, H. G. *J. Chem. Soc., Dalton Trans.* **1999**, 1703. Alt, H. G.; Köppl, A. *Chem. Rev.* **2000**, 100, 1205.

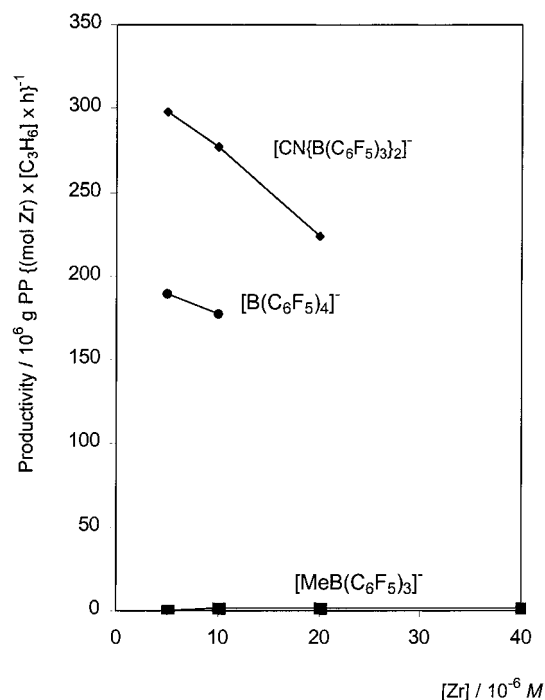


**Figure 10.** Anion effects in propene polymerizations with (SBI)ZrMe<sub>2</sub> catalysts. (1 bar, 20 °C, toluene). For experimental details see Table 4.

Gibson et al.<sup>38</sup> have suggested a simple classification of polymerization catalysts, from “very low” (<10<sup>3</sup> g polymer (mol cat)<sup>-1</sup> h<sup>-1</sup> bar<sup>-1</sup>) to “very high” (>10<sup>6</sup> g polymer (mol cat)<sup>-1</sup> h<sup>-1</sup> bar<sup>-1</sup>), to which even higher categories (10<sup>8</sup> g polymer (mol cat)<sup>-1</sup> h<sup>-1</sup> bar<sup>-1</sup>) could be added. In view of the findings discussed above it seems likely that at least those ethene polymerization catalysts in the “high” classification and above should be suspected of being mass-transport limited, unless it can be demonstrated otherwise. A correlation of ligand structure with catalyst activity in such cases is clearly not very meaningful.

The problem of mass-transport limitation is much reduced in the case of propene polymerizations. Monitoring the amount of polymer produced as a function of catalyst concentration is an easy method for establishing the concentration range where mass-transport limitation may be assumed to be absent for a given reaction temperature.

The results show that there is a very significant dependence of catalyst productivity on the nature of the counteranion, both in the case of ansa-zirconocenes and constrained geometry titanium catalysts, as illustrated in Figures 10 and 11, with catalyst productivities decreasing in the order [CN{B(C<sub>6</sub>F<sub>5</sub>)<sub>3</sub>}<sub>2</sub>]<sup>-</sup> > [B(C<sub>6</sub>F<sub>5</sub>)<sub>4</sub>]<sup>-</sup> ≫ [MeB(C<sub>6</sub>F<sub>5</sub>)<sub>3</sub>]<sup>-</sup>. As in the case of ethene, the activities of the zirconium and titanium catalysts are closely comparable. The titanium system produces atactic polymer and has the advantage of remaining homogeneous, whereas the i-PP produced with the (SBI)Zr catalyst begins to precipitate early in the reaction, although with the short reaction times employed this problem proved not serious.

The system (SBI)ZrMe<sub>2</sub>/activator/AlBu<sub>3</sub> shows an almost linear dependence of catalyst activity on [Zr] (Figure 10), with errors of ±10% or less even for polymerizations conducted at [Zr] = 5 × 10<sup>-7</sup> mol L<sup>-1</sup> (cf. Table 4, entries 2/3: ±3.5%; 4/5: ±3.3%, 7/8: ±9.4%). Under such conditions it is possible to extrapolate to zero catalyst concentration to determine the

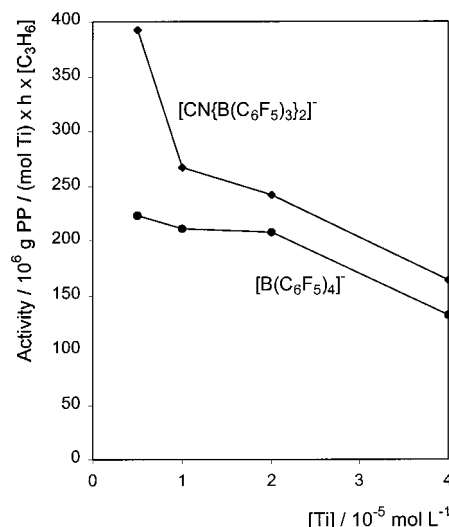


**Figure 11.** Anion effects in propene polymerizations with CGCTiMe<sub>2</sub> catalysts. (1 bar, 20 °C, toluene). For experimental details see Table 4.

“intrinsic” activity of the system. Such an extrapolation allows the quantification of anion and, for a given activator system, of ligand effects, independent of catalyst concentration. For (SBI)-ZrMe<sub>2</sub>/activator/AlBu<sub>3</sub> at 20 °C the intrinsic activity values for [CN{B(C<sub>6</sub>F<sub>5</sub>)<sub>3</sub>}<sub>2</sub>]<sup>-</sup> and [B(C<sub>6</sub>F<sub>5</sub>)<sub>4</sub>]<sup>-</sup> are about 3.2 × 10<sup>8</sup> and 2 × 10<sup>8</sup> g PP (mol Zr)<sup>-1</sup> h<sup>-1</sup> [C<sub>3</sub>H<sub>6</sub>]<sup>-1</sup>, respectively.

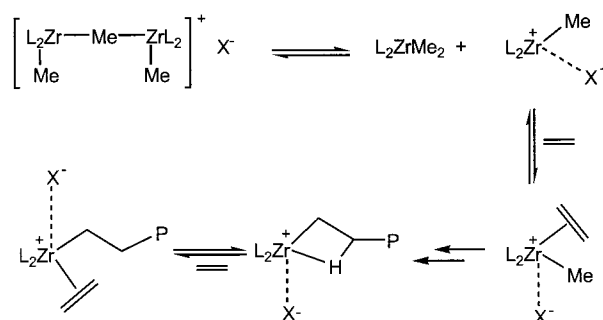
The difference between catalyst activation with CPh<sub>3</sub><sup>+</sup> salts and with B(C<sub>6</sub>F<sub>5</sub>)<sub>3</sub> was particularly pronounced in propene polymerizations. This eliminates the possibility that the observed activities are due to the in situ formation of L<sub>2</sub>ZrMe(μ-Me)B-(C<sub>6</sub>F<sub>5</sub>)<sub>3</sub> from L<sub>2</sub>ZrMe<sub>2</sub> and **1**. Although stoichiometric reactions had demonstrated an extensive decomposition chemistry of the cyanoborate anions, these reactions are slow ≤0.003 s<sup>-1</sup>. With observed propene insertion rates of the order of 10<sup>3</sup> s<sup>-1</sup> chain propagation is ≥10<sup>6</sup> times faster than anion decomposition. This kinetic difference is sufficient to allow thermodynamically labile anions to be used as components in extremely effective polymerization systems.

The marked difference between [CN{B(C<sub>6</sub>F<sub>5</sub>)<sub>3</sub>}<sub>2</sub>]<sup>-</sup> and [B(C<sub>6</sub>F<sub>5</sub>)<sub>4</sub>]<sup>-</sup> was to us initially surprising. The reaction of zirconocene dimethyls with CPh<sub>3</sub><sup>+</sup> salts of both anions leads to identical cationic products [(L<sub>2</sub>ZrMe)<sub>2</sub>(μ-Me)]<sup>+</sup>, and since the reactivity of CPh<sub>3</sub><sup>+</sup> as cation generating agent is unlikely to be affected by the counteranion, these will be formed in equal concentrations. The weakly coordinating anion [B(C<sub>6</sub>F<sub>5</sub>)<sub>4</sub>]<sup>-</sup> is not able to enter the coordination sphere of [(L<sub>2</sub>ZrMe)<sub>2</sub>(μ-Me)]<sup>+</sup>, and polymerization activity could therefore be expected to depend simply on the degree of dissociation of [(L<sub>2</sub>ZrMe)<sub>2</sub>(μ-Me)]<sup>+</sup> in the presence of monomer to generate [L<sub>2</sub>ZrMe(olefin)]<sup>+</sup> + L<sub>2</sub>ZrMe<sub>2</sub>. On that basis, a further reduction in anion nucleophilicity below that of [B(C<sub>6</sub>F<sub>5</sub>)<sub>4</sub>]<sup>-</sup> might be expected to involve little change in the transition state and, hence, have no bearing on the active species concentration or on the rate of chain growth. The results show, however, that this is not the case, and even very weakly coordinating anions are intimately associated with the cations during the olefin insertion step. It seems likely, therefore, that the binuclear ion pair [(L<sub>2</sub>ZrMe)<sub>2</sub>(μ-Me)]<sup>+</sup>...X<sup>-</sup> first produces L<sub>2</sub>ZrMe<sub>2</sub> + [L<sub>2</sub>ZrMe<sup>+</sup>...X<sup>-</sup>], followed by reaction of the mononuclear ion pair with alkene and displacement of the anion from the coordination sphere of the metal (Scheme 4). The activation barrier of this process would of course be lowered by reducing anion nucleophilicity. We interpret the observed activity enhancement seen with **1** as a reflection of the more extensive delocalization of the negative

(38) Britovsek, G. J. P.; Gibson, V. C.; Wass, D. F. *Angew. Chem., Int. Ed.* **1999**, *38*, 429.



Scheme 4

**Table 6.** Rates of Migratory Monomer Insertions and Activation Energies for Propene Polymerizations with at 293 K<sup>a</sup>

activator	activity <sup>b</sup>	monomer insertion frequency/s <sup>-1</sup>	$\Delta G^\ddagger$ /kJ mol <sup>-1</sup>
<b>1</b>	297.5	1967	53.2
[CPh <sub>3</sub> ][B(C <sub>6</sub> F <sub>5</sub> ) <sub>4</sub> ]	189.3	1252	54.3
B(C <sub>6</sub> F <sub>5</sub> ) <sub>3</sub>	1.60	10.6	66.0
	3.77	25	63.9

<sup>a</sup> Catalyst (SBI)ZrMe<sub>2</sub>/activator/AlBu<sub>3</sub> 1:1:200. <sup>b</sup> In 10<sup>6</sup> g PP (mol Zr)<sup>-1</sup> [C<sub>3</sub>H<sub>6</sub>]<sup>-1</sup> h<sup>-1</sup>.

charge in the diborate [CN{B(C<sub>6</sub>F<sub>5</sub>)<sub>3</sub>}<sub>2</sub>]<sup>-</sup> which helps to weaken cation–anion interactions.

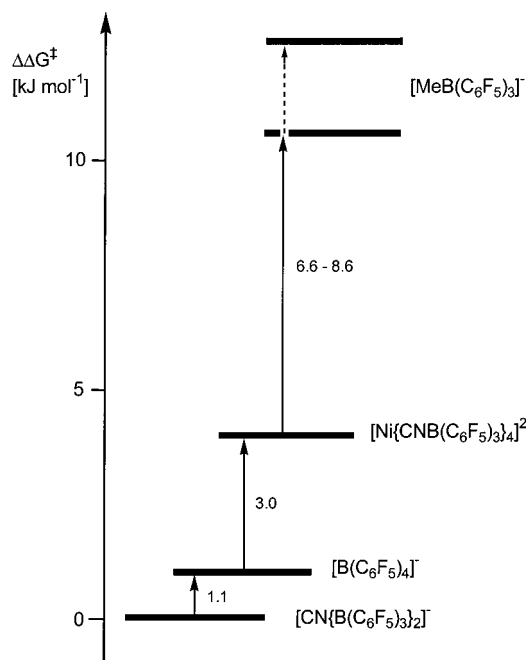
The importance of cation–anion association may be gauged from a consideration of the electrostatic binding energy  $E_C$  and the association constant  $K_{\text{ass}}$  for the process  $C^+ + A^- = C^+A^-$ . According to the Eigen–Denison–Ramsey–Fuoss (EDRF) model,<sup>39</sup> for two monovalent ions in a solvent of low dielectric constant such as toluene ( $\epsilon = 2.379$  at 25 °C) at a distance of 8 Å,  $K_{\text{ass}} = 7.9 \times 10^6$  m<sup>3</sup> mol<sup>-1</sup>. The attraction between a monocation and a dianion, as in [L<sub>2</sub>ZrMe<sup>+</sup>...Ni{CNB(C<sub>6</sub>F<sub>5</sub>)<sub>3</sub>}<sub>4</sub>]<sup>2-</sup>, is orders of magnitude higher,  $K_{\text{ass}}$  (at 8 Å) =  $4.9 \times 10^{19}$  m<sup>3</sup> mol<sup>-1</sup>. Even allowing for the difficulty of determining the appropriate inter-ion distance in the case of bulky, nonspherical anion structures such as [Ni{CNB(C<sub>6</sub>F<sub>5</sub>)<sub>3</sub>}<sub>4</sub>]<sup>2-</sup>, it is clear that dianions are bound considerably more strongly than monoanions, in line with the reduced catalytic activity of systems activated with **4c** or **5c**, compared to **1**.

From the observed propene polymerization activities the differences in activation barriers  $\Delta\Delta G^\ddagger$  may be calculated as a function of the counteranion (Table 6). For the [CN{B(C<sub>6</sub>F<sub>5</sub>)<sub>3</sub>}<sub>2</sub>]<sup>-</sup> anion system a monomer insertion rate of  $k = 1967$  s<sup>-1</sup> was found, corresponding to  $\Delta G^\ddagger = 53.2$  kJ mol<sup>-1</sup>. While less importance should be attached to the absolute  $\Delta G^\ddagger$  value obtained by such a simple approximation, the differences between activation barriers are significant (Figure 12): the activation energies for the [B(C<sub>6</sub>F<sub>5</sub>)<sub>4</sub>]<sup>-</sup> and [Ni{CNB(C<sub>6</sub>F<sub>5</sub>)<sub>3</sub>}<sub>4</sub>]<sup>2-</sup>-based systems are higher by 1.1 and 4.1 kJ mol<sup>-1</sup>, respectively. The B(C<sub>6</sub>F<sub>5</sub>)<sub>3</sub>-activated catalyst, although not evaluated on strictly the same time scale, shows a further barrier increase by 6.6–8.6 kJ mol<sup>-1</sup>. Evidently there is a very significant difference in activation barrier between the group of three “noncoordinating” borates, **1**, [B(C<sub>6</sub>F<sub>5</sub>)<sub>4</sub>]<sup>-</sup> and **4c**, and zwitterion-forming [MeB(C<sub>6</sub>F<sub>5</sub>)<sub>3</sub>]<sup>-</sup>.

## Conclusions

Adducts between B(C<sub>6</sub>F<sub>5</sub>)<sub>3</sub> and basic anions, in this case CN<sup>-</sup> or [M{CN}A]<sub>4</sub><sup>2-</sup>, give rise to new, very weakly coordinating

(39) Gordon, J. E. *The Organic Chemistry of Electrolyte Solutions*, Wiley: New York, 1975; p 372ff. The association constant is given by  $K_{\text{ass}} = [4\pi N_A r^3 / 3000] e^b$ , where  $b = (|z^+ z^-| e^2) / 4\pi \epsilon_0 kT$ ,  $r$  = distance between ions;  $\epsilon$  = dielectric constant of the solvent.

**Figure 12.** Differences in activation barriers  $\Delta\Delta G^\ddagger$  for propene polymerizations with the catalyst system (SBI)ZrMe<sub>2</sub>/activator/AlBu<sub>3</sub> at 20 °C as a function of anion structure [kJ mol<sup>-1</sup>]. The values for [MeB(C<sub>6</sub>F<sub>5</sub>)<sub>3</sub>]<sup>-</sup> were estimated from reactions of 10–30 min duration.

anions suitable as counteranions in metallocene-based polymerization catalysts. A general protocol has been developed to define the concentration range for which mass-transport limitation is absent and to quantify the effect of the counteranion on catalyst activity. Ethene polymerizations were found to be strongly mass-transport limited for ethene pressures of 1–7 bar, to the extent that no meaningful correlation can be drawn between catalyst productivity and ligand or anion effects. By contrast, propene polymerizations with zirconocene and constrained geometry titanium catalysts confirmed that charge delocalization in cyanoborates gives anions with reduced nucleophilicity and results in enhanced catalytic activities. Activation barriers for propene polymerizations increase in the order [CN{B(C<sub>6</sub>F<sub>5</sub>)<sub>3</sub>}<sub>2</sub>]<sup>-</sup> < [B(C<sub>6</sub>F<sub>5</sub>)<sub>4</sub>]<sup>-</sup> < [Ni{CNB(C<sub>6</sub>F<sub>5</sub>)<sub>3</sub>}<sub>4</sub>]<sup>2-</sup> << [MeB(C<sub>6</sub>F<sub>5</sub>)<sub>3</sub>]<sup>-</sup>. In the [CGCTiMe]<sup>+</sup>X<sup>-</sup> system, the polymer molecular weight is strongly anion-dependent. The observed thermodynamic lability of cyanoborates in stoichiometric reactions is kinetically unimportant under polymerization reactions, with propagation rates  $\geq 10^6$  times faster than anion decomposition.

## Experimental Section

**General Methods.** All manipulations were performed under dinitrogen using Schlenk techniques. Solvents were distilled under nitrogen over sodium benzophenone (diethyl ether, THF), sodium (low-sulfur toluene), sodium–potassium alloy (light petroleum, bp 40–60 °C), or CaH<sub>2</sub> (dichloromethane). NMR solvents were dried over activated 4Å molecular sieves and degassed by several freeze–thaw cycles. 1,2-Difluorobenzene was predried over CaH<sub>2</sub>, stored over 4Å molecular sieves, and degassed by several freeze–thaw cycles. NMR spectra were recorded using Bruker ARX250 and DPX300 spectrometers. Chemical shifts are reported in ppm. <sup>1</sup>H NMR spectra were referenced to the residual solvent protons of the deuterated solvent used; <sup>13</sup>C NMR spectra (75.4 MHz) were referenced internally to the D-coupled <sup>13</sup>C resonances of the NMR solvent. <sup>19</sup>F (282.2 MHz) and <sup>11</sup>B (96.29 MHz) NMR spectra were referenced externally to CFCl<sub>3</sub> and BF<sub>3</sub>·OEt<sub>2</sub>, respectively. The compounds B(C<sub>6</sub>F<sub>5</sub>)<sub>3</sub>,<sup>9a,b</sup> B(C<sub>6</sub>F<sub>5</sub>)<sub>3</sub>·Et<sub>2</sub>O,<sup>9c</sup> [CPh<sub>3</sub>][B(C<sub>6</sub>F<sub>5</sub>)<sub>3</sub>],<sup>21b,41</sup>

(40) Samuel, E.; Rausch, M. D. *J. Am. Chem. Soc.* **1973**, *95*, 6263.



$\text{Cp}_2\text{ZrMe}_2$ ,<sup>40</sup> (SBI)ZrMe<sub>2</sub>,<sup>22</sup> CGCTiMe<sub>2</sub>,<sup>7d</sup> and CGCTi(CH<sub>2</sub>Ph)<sub>2</sub>,<sup>7d</sup> were prepared according to literature procedures; other reagents were used as purchased. Nitrogen, argon, ethene (BOC, 99.5%), and propene (BOC, 99%) were purified by passing through columns of CaCl<sub>2</sub>, supported P<sub>2</sub>O<sub>5</sub> with moisture indicator, and 4 Å molecular sieves. The thermal analysis of polymers was carried out using a Mettler differential scanning calorimeter (DSC12E) set at a heating rate of 10 °C/min under N<sub>2</sub> atmosphere.

**Preparation of [CPh<sub>3</sub>][CN{B(C<sub>6</sub>F<sub>5</sub>)<sub>3</sub>}<sub>2</sub>] (1).** B(C<sub>6</sub>F<sub>5</sub>)<sub>3</sub>·Et<sub>2</sub>O (20.1 g, 34 mmol) was combined with 1.10 g (17 mmol) KCN. Diethyl ether (150 mL) was added and the reaction stirred overnight. The solids slowly dissolved to give a clear solution after 12 h. The solvent was removed in vacuo, and the residue was dried to give a colorless foam. Triphenylchloromethane (5.68 g, 20.4 mmol) was added, followed by 200 mL of dichloromethane. The reaction was stirred for 1 h, filtered, and concentrated to ~40 mL. Addition of light petroleum and cooling to -20 °C produced yellow crystals, yield (two fractions) 10 g (7.7 mmol, 45%). Anal. Calcd for C<sub>56</sub>H<sub>15</sub>B<sub>2</sub>F<sub>30</sub>N: C, 52.0; H, 1.2; N, 1.1. Found: C, 52.1; H, 1.3; N, 0.8. <sup>1</sup>H NMR (300.13 MHz, CDCl<sub>3</sub>, 293 K) δ 8.26 (t, 3H, *J* = 7.7 Hz, *p*-H), 7.87 ("t", 6H, *J* = 7.7 Hz, *m*-H), 7.66 (d, 6H, *J* = 7.2 Hz, *o*-H). <sup>13</sup>C{<sup>1</sup>H} NMR (75.47 MHz, CDCl<sub>3</sub>, 293 K) δ 210.89 (CPh<sub>3</sub>), 148.17 (d, *J*<sub>C-F</sub> = 253 Hz, *o*-C, C<sub>6</sub>F<sub>5</sub>), 143.88 (*p*-C, CPh<sub>3</sub>), 142.53 (*m*-C, CPh<sub>3</sub>), 140.09 (d, *J*<sub>C-F</sub> = 203 Hz, *p*-C, C<sub>6</sub>F<sub>5</sub>), 136.79 (d, *J*<sub>C-F</sub> = 227 Hz, *m*-C, C<sub>6</sub>F<sub>5</sub>), 130.85 (*o*-C, CPh<sub>3</sub>). <sup>19</sup>F NMR (282.4 MHz, CDCl<sub>3</sub>, 293 K) δ -133.29 (d, *J*<sub>F-F</sub> = 21.2 Hz, *o*-F), -134.40 (d, *J*<sub>F-F</sub> = 20.4 Hz, *o*-F), -158.68 (t, *J*<sub>F-F</sub> = 21.6 Hz, *p*-F), -158.85 (t, *J*<sub>F-F</sub> = 20 Hz, *p*-F), -165.14 (t, *J*<sub>F-F</sub> = 16.5 Hz, *m*-F), -165.47 (t, *J*<sub>F-F</sub> = 20.9 Hz, *m*-F). <sup>11</sup>B NMR (96.29 MHz, CDCl<sub>3</sub>, 293 K) δ -11.94 (br, N-B), -21.68 (C-B). Infrared (Nujol mull) 2305 cm<sup>-1</sup> (ν<sub>CN</sub>).

**Preparation of [CPh<sub>3</sub>][ClB(C<sub>6</sub>F<sub>5</sub>)<sub>3</sub>] (2).** Ph<sub>3</sub>CCl (0.23 g, 0.84 mmol) and B(C<sub>6</sub>F<sub>5</sub>)<sub>3</sub>·Et<sub>2</sub>O (1.0 g, 1.7 mmol) were dissolved in CH<sub>2</sub>Cl<sub>2</sub> (30 mL). The solution was stirred for 2 h, followed by removal of the solvent in vacuo. The product was an orange-yellow solid. Crystals suitable for single-crystal X-ray determination were obtained by layering a CH<sub>2</sub>Cl<sub>2</sub> solution of the product with light petroleum at 5 °C; yield 0.27 g (0.35 mmol, 42%). Anal. Calcd for C<sub>37</sub>H<sub>15</sub>BClF<sub>15</sub>: C, 56.2; H, 1.9; Cl, 4.5. Found: C, 56.3; H, 2.0; Cl, 4.5. <sup>1</sup>H NMR (300 MHz, 300 K, CD<sub>2</sub>Cl<sub>2</sub>) δ 8.26 (t, 3H, *J* = 7.5 Hz, *p*-H), 7.87 ("t", 6H, *J* = 7.9 Hz, *m*-H), 7.68 (d, 6H, *J* = 8.3 Hz, *o*-H). <sup>19</sup>F NMR (282 MHz, 300 K, CD<sub>2</sub>Cl<sub>2</sub>) δ -130.86 (d, *J*<sub>FF</sub> = 19.7 Hz, *o*-F), -160.54 (br, *p*-F), -165.18 (br, *m*-F).

**[PhNMe<sub>2</sub>H][HSO<sub>3</sub>{OB(C<sub>6</sub>F<sub>5</sub>)<sub>3</sub>}] (3).** To a solution of B(C<sub>6</sub>F<sub>5</sub>)<sub>3</sub>·Et<sub>2</sub>O (2.0 g, 3.4 mmol) in CH<sub>2</sub>Cl<sub>2</sub> (50 mL) was added [PhNMe<sub>2</sub>H][HSO<sub>4</sub>] (0.29 g, 0.85 mmol). The solution was stirred vigorously for 12 h, followed by removal of the solvent in vacuo. The resulting solid was washed with light petroleum to remove any free borane; yield: 0.39 g (0.57 mmol, 67%). Anal. Calcd for C<sub>26</sub>H<sub>13</sub>BF<sub>15</sub>NO<sub>4</sub>S: C, 42.7; H, 1.8; N, 1.9. Found: C, 43.1; H, 2.1; N, 1.8. <sup>1</sup>H NMR (300 MHz, 300 K, CD<sub>3</sub>OD) δ 3.31 (s, 12 H, Me), 7.58–7.63 (m, 10 H, Ph); <sup>19</sup>F NMR (282 MHz, 300 K, CD<sub>3</sub>OD) δ -133.9 (d, *J*<sub>FF</sub> = 20.6 Hz, *o*-F), -161.24 (t, *J*<sub>FF</sub> = 20.9 Hz, *p*-F), -166.4 (t, *J*<sub>FF</sub> = 20.6 Hz, *m*-F). <sup>11</sup>B (80 MHz, 300 K, CD<sub>3</sub>OD) δ -1.99.

**K<sub>2</sub>[Ni{CNB(C<sub>6</sub>F<sub>5</sub>)<sub>3</sub>}<sub>4</sub>] (4a).** To a solution of B(C<sub>6</sub>F<sub>5</sub>)<sub>3</sub>·Et<sub>2</sub>O (2.0 g, 3.4 mmol) in CH<sub>2</sub>Cl<sub>2</sub> (50 mL) was added K<sub>2</sub>[Ni(CN)<sub>4</sub>] (0.18 g, 0.85 mmol). The mixture was stirred for 12 h. The white solid product was washed with light petroleum to remove any free borane. The compound was used without further purification; yield 1.55 g (0.68 mmol, 80%). <sup>19</sup>F NMR (282 MHz, 298 K, CD<sub>3</sub>OD) δ -135.74 (d, *J*<sub>FF</sub> = 19.7 Hz, *o*-F), -162.74 (t, *J*<sub>FF</sub> = 19.7 Hz, *p*-F), -168.19 (t, *J*<sub>FF</sub> = 19.7 Hz, *m*-F). <sup>11</sup>B NMR (96 MHz, 300 K, CD<sub>3</sub>OD) δ -2.34. Infrared (Nujol mull) 2236 cm<sup>-1</sup> (ν<sub>CN</sub>).

**[PhNMe<sub>2</sub>H]<sub>2</sub>[Ni{CNB(C<sub>6</sub>F<sub>5</sub>)<sub>3</sub>}<sub>4</sub>] (4b).** To a solution of [PhNMe<sub>2</sub>H]Cl (1.3 g, 2.1 mmol) in CH<sub>2</sub>Cl<sub>2</sub> (50 mL) was added **4a** (2.68 g, 1.05 mmol). The mixture was stirred for 12 h and filtered. The solvent was removed from the filtrate in vacuo. The white solid residue was washed with light petroleum. Crystals suitable for single-crystal X-ray determination were obtained by layering a CH<sub>2</sub>Cl<sub>2</sub> solution of the product

with light petroleum at 5 °C in the presence of traces of acetone; yield 1.68 g (6.8 mmol, 55%). Anal. Calcd for C<sub>92</sub>H<sub>24</sub>B<sub>4</sub>F<sub>60</sub>N<sub>6</sub>Ni·2(CH<sub>3</sub>)<sub>2</sub>CO: C, 42.0; H, 1.6; N, 3.6. Found: C, 42.2; H, 1.4; N, 3.2. <sup>1</sup>H NMR (300 MHz, 298 K, CD<sub>2</sub>Cl<sub>2</sub>) δ 3.28 (s, 6 H, Me), 7.59 (m, 5 H, Ph). <sup>19</sup>F (282 MHz, 300 K, CD<sub>2</sub>Cl<sub>2</sub>) δ -133.68 (d, *J*<sub>FF</sub> = 20.6 Hz, *o*-F), -160.63 (t, *J*<sub>FF</sub> = 20.6 Hz, *p*-F), -166.36 (t, *J*<sub>FF</sub> = 20.6 Hz, *m*-F). Infrared (Nujol mull) 2239 cm<sup>-1</sup> (ν<sub>CN</sub>).

**[CPh<sub>3</sub>]<sub>2</sub>[Ni{CNB(C<sub>6</sub>F<sub>5</sub>)<sub>3</sub>}<sub>4</sub>] (4c).** To a solution of Ph<sub>3</sub>CCl (0.58 g, 2.1 mmol) and B(C<sub>6</sub>F<sub>5</sub>)<sub>3</sub>·Et<sub>2</sub>O (2.02 g, 3.0 mmol) in CH<sub>2</sub>Cl<sub>2</sub> (50 mL) was added K<sub>2</sub>[Ni(CN)<sub>4</sub>] (0.21 g, 0.75 mmol). The mixture was stirred for 12 h and filtered. Removal of the solvent in vacuo afforded an orange-yellow solid which was washed with light petroleum to remove any free borane. Recrystallization by layering a CH<sub>2</sub>Cl<sub>2</sub> solution of the product with light petroleum at 5 °C gave **4c**·2CH<sub>2</sub>Cl<sub>2</sub>; the crystals were suitable for single-crystal X-ray diffraction; yield 0.80 g (3.0 mmol, 34%). Anal. Calcd for C<sub>114</sub>H<sub>30</sub>B<sub>4</sub>F<sub>60</sub>N<sub>4</sub>Ni·2CH<sub>2</sub>Cl<sub>2</sub>: C, 48.6; H, 1.2; N, 2.0. Found: C, 49.0; H, 1.1; N, 2.1. <sup>1</sup>H NMR (250 MHz, 298 K, CD<sub>2</sub>Cl<sub>2</sub>) δ 7.69 (d, 6 H, *o*-H), 7.91 (t, 6 H, *J* = 8.1 Hz, *m*-H), 8.29 (t, 1 H, *J* = 7.4 Hz, *p*-H); <sup>19</sup>F NMR (282 MHz, 300 K, CD<sub>2</sub>Cl<sub>2</sub>) δ -134.64 (d, *o*-F), -159.56 (t, *p*-F), -165.82 (t, *m*-F). Infrared (Nujol mull) 2234 cm<sup>-1</sup> (ν<sub>CN</sub>).

**K<sub>2</sub>[Pd{CNB(C<sub>6</sub>F<sub>5</sub>)<sub>3</sub>}<sub>4</sub>] (5a).** To a solution of B(C<sub>6</sub>F<sub>5</sub>)<sub>3</sub>·Et<sub>2</sub>O (2.40 g, 4.1 mmol) in CH<sub>2</sub>Cl<sub>2</sub> (50 mL) was added K<sub>2</sub>[Pd(CN)<sub>4</sub>] (0.29 g, 1.02 mmol). The mixture was stirred vigorously for 12 h, affording a white solid which was washed with light petroleum to remove any borane; yield 1.91 g (0.82 mmol, 80%). The compound was used without further purification. <sup>19</sup>F NMR (282 MHz, 300 K, CD<sub>3</sub>OD) δ -132.63 to -130.37 (m, *o*-F), -158.6 to -157.21 (m, *p*-F), -164.79 to -163.58 (m, *m*-F).

**[CPh<sub>3</sub>]<sub>2</sub>[Pd{CNB(C<sub>6</sub>F<sub>5</sub>)<sub>3</sub>}<sub>4</sub>] (5c).** To a solution of Ph<sub>3</sub>CCl (0.43 g, 1.54 mmol) in CH<sub>2</sub>Cl<sub>2</sub> (50 mL) was added K<sub>2</sub>[Pd{CNB(C<sub>6</sub>F<sub>5</sub>)<sub>3</sub>}<sub>4</sub>] (1.80 g, 0.78 mmol). The mixture was stirred vigorously for 12 h and filtered. The solvent was removed in vacuo to give an orange-yellow solid which was washed with light petroleum. Crystals of **5c**·2CH<sub>2</sub>Cl<sub>2</sub> suitable for single-crystal X-ray diffraction were obtained by layering a CH<sub>2</sub>Cl<sub>2</sub> solution of the product with light petroleum at 5 °C. They are prone to solvent loss; yield 1.05 g (0.38 mmol, 49%). Anal. Calcd for C<sub>114</sub>H<sub>30</sub>B<sub>4</sub>F<sub>60</sub>N<sub>4</sub>Pd·1.5CH<sub>2</sub>Cl<sub>2</sub>: C, 48.3; H, 1.2; N, 1.9. Found: C, 47.8; H, 1.4; N, 1.8. <sup>1</sup>H NMR (300 MHz, 300 K, CD<sub>2</sub>Cl<sub>2</sub>) δ 8.27 (t, 3 H, *p*-H), 7.88 (t, 6 H, *m*-H), 7.67 (d, 6 H, *o*-H); <sup>19</sup>F NMR (282.4 MHz, 300 K, CD<sub>2</sub>Cl<sub>2</sub>) δ -134.87 (d, *J*<sub>FF</sub> = 20.6 Hz, *o*-F), -160.41 (t, *J*<sub>FF</sub> = 20.6 Hz, *m*-F), -166.57 (t, *J*<sub>FF</sub> = 20.6 Hz, *p*-F). <sup>11</sup>B NMR (80 MHz, 300 K, CD<sub>2</sub>Cl<sub>2</sub>) δ -12.81. Infrared (Nujol mull) 2243 cm<sup>-1</sup> (ν<sub>CN</sub>).

**Preparation of Cp''<sub>2</sub>Zr(Me)NCB(C<sub>6</sub>F<sub>5</sub>)<sub>3</sub> (6).** To a suspension of 0.64 g (0.49 mmol) **1** in 10 mL of toluene was added a solution of AlMe<sub>3</sub> in toluene (4.9 mL, 3.9 mmol), immediately followed by solution of Cp''<sub>2</sub>ZrMe<sub>2</sub> (4.9 mL, 0.1 mol/L, 0.49 mmol). There was a rapid color change from the oily orange trityl salt suspension to a yellow oily suspension. After being stirred for 30 min the yellow suspension dissolved to give a pale yellow solution. Cooling to 5 °C overnight yielded crystals of **6**·toluene suitable for X-ray diffraction; yield 0.3 g (0.26 mmol, 53%). Anal. Calcd for C<sub>42</sub>H<sub>45</sub>BF<sub>15</sub>NSi<sub>4</sub>Zr·C<sub>7</sub>H<sub>8</sub>: C, 50.9; H, 4.6; N, 1.2. Found: C, 50.9; H, 4.5; N, 1.0. <sup>1</sup>H NMR (300.13 MHz, CD<sub>2</sub>Cl<sub>2</sub>, 293 K) δ 7.12 (s, 2H, 2-C<sub>5</sub>H<sub>3</sub>), 6.35 (t, 2H, *J* = 2 Hz, C<sub>5</sub>H<sub>3</sub>), 6.28 (t, 2H, *J* = 2 Hz, C<sub>5</sub>H<sub>3</sub>), 0.54 (s, 3H, Zr-CH<sub>3</sub>), 0.19 (s, 18H, Si(CH<sub>3</sub>)<sub>3</sub>), 0.13 (s, 18H, Si(CH<sub>3</sub>)<sub>3</sub>). <sup>13</sup>C NMR (75.47 MHz, CD<sub>2</sub>Cl<sub>2</sub>, 293 K) δ 137.02 (2-C<sub>5</sub>H<sub>3</sub>), 130.59 (C<sub>5</sub>H<sub>3</sub>), 127.60 (C<sub>5</sub>H<sub>3</sub>), 120.01 (C<sub>5</sub>H<sub>3</sub>), 118.88 (C<sub>5</sub>H<sub>3</sub>), 47.58 (Zr-CH<sub>3</sub>), -0.21 (Si(CH<sub>3</sub>)<sub>3</sub>), -0.39 (Si(CH<sub>3</sub>)<sub>3</sub>). <sup>11</sup>B NMR (96.29 MHz, CD<sub>2</sub>Cl<sub>2</sub>, 293 K) δ -19.57.

**NMR Studies.** Samples for studies at room temperature were prepared from C<sub>6</sub>D<sub>6</sub> stock solutions of the corresponding zirconocene (0.004 mol/L, Cp<sub>2</sub>ZrMe<sub>2</sub>, *rac*-Me<sub>2</sub>Si(Ind)<sub>2</sub>ZrMe<sub>2</sub>, Cp''<sub>2</sub>ZrMe<sub>2</sub>), and the activators (0.002 mol/L). Stock solutions were prepared and handled in a glovebox. NMR samples were prepared by pipetting the required volumina of the zirconocene and borate solutions using an Eppendorf pipet, accuracy ±2 μL. The total zirconocene concentration ([Zr]<sub>tot</sub>) in the NMR tube was kept under ~3 mmol/L (typically 0.6 mmol/L < [Zr]<sub>tot</sub> < 2.5 mmol/L) to prevent the formation of higher aggregates and the precipitation of ionic species as "orange-red oils". The solubility of [CPh<sub>3</sub>]<sub>2</sub>[Ni{CNB(C<sub>6</sub>F<sub>5</sub>)<sub>3</sub>}<sub>4</sub>] in benzene was insufficient, and up to 20 vol % of *o*-C<sub>6</sub>H<sub>4</sub>F<sub>2</sub> had to be added; in this way samples of

(41) Bochmann, M.; Lancaster, S. J. *J. Organomet. Chem.* **1992**, 434, C1.

$[\text{Zr}]_{\text{tot}} = \sim 3 \text{ mmol/L}$  were prepared. The samples studied at lower temperatures in  $\text{CD}_2\text{Cl}_2$  were prepared by weighing each component directly into the NMR tube (glovebox), followed by the addition of the cooled solvent. The polar solvent allowed concentrations of  $[\text{Zr}]_{\text{tot}} = 55 \text{ mmol/L}$ . Assignments are based on  $^1\text{H}$ ,  $^1\text{H}-^1\text{H}$  COSY,  $^{13}\text{C}$  and  $^1\text{H}-^{13}\text{C}$  HETCOR spectra.

**The System  $\text{L}_2\text{ZrMe}_2/[\text{CPh}_3][\text{B}(\text{C}_6\text{F}_5)_4]$ .** The reactions of the zirconocene complexes  $\text{L}_2\text{ZrMe}_2 = \text{Cp}_2\text{ZrMe}_2$  and  $\text{rac-Me}_2\text{Si}(\text{Ind})_2\text{ZrMe}_2$  with  $[\text{CPh}_3][\text{B}(\text{C}_6\text{F}_5)_4]$  were studied at various Zr:B ratios. Addition of  $\text{L}_2\text{ZrMe}_2$  to an excess of  $[\text{CPh}_3][\text{B}(\text{C}_6\text{F}_5)_4]$  gives the binuclear zirconocene cations  $[(\text{L}_2\text{ZrMe})_2(\mu\text{-Me})^+\cdots\text{B}(\text{C}_6\text{F}_5)_4]^-$  for both zirconocene systems in benzene solution at 298 K. The mononuclear product  $[\text{L}_2\text{ZrMe}^+\cdots\text{B}(\text{C}_6\text{F}_5)_4]^-$  is detected after a few minutes.

**$[(\text{Cp}_2\text{ZrMe})_2(\mu\text{-Me})^+\cdots\text{B}(\text{C}_6\text{F}_5)_4]^-$ .**<sup>21a</sup> From  $\text{C}_6\text{D}_6$  solutions of  $\text{Cp}_2\text{ZrMe}_2$  (0.004 mol/L, 220  $\mu\text{L}$ ) and  $[\text{CPh}_3][\text{B}(\text{C}_6\text{F}_5)_4]$  (220  $\mu\text{L}$ , 0.002 mol/L),  $[\text{Zr}] = 0.002 \text{ mol/L}$ .  $[(\text{Cp}_2\text{ZrMe})_2(\mu\text{-Me})^+\cdots\text{B}(\text{C}_6\text{F}_5)_4]^-$  was detected as the sole product.  $^1\text{H}$  NMR (300 MHz,  $\text{C}_6\text{D}_6$ , 298 K)  $\delta$  5.56 (s, 20H,  $\text{C}_5\text{H}_5$ ), -0.13 (s, 6H, Zr-Me), -1.27 (s, 3H,  $\mu\text{-Me}$ ).  **$[\text{Cp}_2\text{ZrMe}^+\cdots\text{B}(\text{C}_6\text{F}_5)_4]^-$ .**  $\text{C}_6\text{D}_6$  solutions of  $\text{Cp}_2\text{ZrMe}_2$  (0.004 mol/L, 100  $\mu\text{L}$ ) and  $\text{Ph}_3\text{C}^+\text{B}(\text{C}_6\text{F}_5)_4^-$  (0.002 mol/L, 300  $\mu\text{L}$ ) were transferred into the NMR tube ( $[\text{Zr}] = 0.001 \text{ mol/L}$ ). Initially formed  $[(\text{Cp}_2\text{ZrMe})_2(\mu\text{-Me})^+\cdots\text{B}(\text{C}_6\text{F}_5)_4]^-$  reacts with excess trityl borate to give  $[\text{Cp}_2\text{ZrMe}^+\cdots\text{B}(\text{C}_6\text{F}_5)_4]^-$ .  $^1\text{H}$  NMR (300 MHz,  $\text{C}_6\text{D}_6$ , 298 K)  $\delta$  5.20 (s, 20H, Cp), 0.15 (s, 3H, Zr-Me).

**$\{[(\text{SBI})\text{ZrMe}]_2(\mu\text{-Me})^+\cdots\text{B}(\text{C}_6\text{F}_5)_4\}^-$ .**<sup>21a</sup> From (SBI)ZrMe<sub>2</sub> (220  $\mu\text{L}$ , 0.004 mol/L) and  $[\text{CPh}_3][\text{B}(\text{C}_6\text{F}_5)_4]$  (220  $\mu\text{L}$ , 0.002 mol/L) in  $\text{C}_6\text{D}_6$ ,  $[\text{Zr}] = 0.002 \text{ mol/L}$ . After a few minutes  $\{[(\text{SBI})\text{ZrMe}]_2(\mu\text{-Me})^+\cdots\text{B}(\text{C}_6\text{F}_5)_4\}^-$  is observed as the sole product.  $^1\text{H}$  NMR (300 MHz,  $\text{C}_6\text{D}_6$ , 298 K)  $\delta$  -0.96 (s, 6, Zr-Me, *rac*-like), -1.01 (s, 6, Zr-Me, *meso*-like), -2.91 (s, 3,  $\mu\text{-Me}$ , *rac*-like), -3.10 (s, 3,  $\mu\text{-Me}$ , *meso*-like). The overlapping indenyl signals are not listed.

**$[(\text{SBI})\text{ZrMe}^+\cdots\text{B}(\text{C}_6\text{F}_5)_4]^-$ .** From (SBI)ZrMe<sub>2</sub> (100  $\mu\text{L}$ , 0.004 mol/L) and  $[\text{CPh}_3][\text{B}(\text{C}_6\text{F}_5)_4]$  (500  $\mu\text{L}$ , 0.002 mol/L) in  $\text{C}_6\text{D}_6$ ,  $[\text{Zr}] = 6.67 \times 10^{-4} \text{ mol/L}$ . The initially formed  $\{[(\text{SBI})\text{ZrMe}]_2(\mu\text{-Me})^+\cdots\text{B}(\text{C}_6\text{F}_5)_4\}^-$  reacts slowly to  $[(\text{SBI})\text{ZrMe}^+\cdots\text{B}(\text{C}_6\text{F}_5)_4]^-$ . The reaction is complete after 65 min. NMR spectra were measured every 5 min. A pseudo-first-order rate constant  $k = 3 \times 10^{-4} \text{ s}^{-1}$  was determined by evaluation of the integrals of the two observed zirconocene species.  $^1\text{H}$  NMR (300 MHz,  $\text{C}_6\text{D}_6$ , 298 K)  $\delta$  5.15 (br, 2,  $\alpha\text{-C}_5\text{H}_2$ ), 0.32 (br, 6, Si-Me), -0.79 (s, 3, Zr-Me).

**The System  $\text{L}_2\text{ZrMe}_2/\mathbf{1}$ .** Mixing  $\text{C}_6\text{D}_6$  solutions of  $\text{Cp}_2\text{ZrMe}_2$  (220  $\mu\text{L}$ , 0.004 mol/L) and **1** (220  $\mu\text{L}$ , 0.002 mol/L) at 25  $^\circ\text{C}$  gives  $[(\text{Cp}_2\text{ZrMe})_2(\mu\text{-Me})^+\cdots(\text{C}_6\text{F}_5)_3\text{BCNB}(\text{C}_6\text{F}_5)_3]^-$  together with decomposition products ( $[\text{Zr}]_{\text{tot}} = 0.002 \text{ mol/L}$ ). Decomposition is complete after 5 min. The products  $\text{Cp}_2\text{ZrMe}(\mu\text{-Me})\text{B}(\text{C}_6\text{F}_5)_3$  and one other species, assigned to  $\text{Cp}_2\text{ZrMe}(\mu\text{-NC})\text{B}(\text{C}_6\text{F}_5)_3$ , were detected. The ion pair  $\{[(\text{SBI})\text{ZrMe}]_2(\mu\text{-Me})^+\cdots(\text{C}_6\text{F}_5)_3\text{BCNB}(\text{C}_6\text{F}_5)_3\}^-$  is more stable in  $\text{C}_6\text{D}_6$ .  **$[(\text{Cp}_2\text{ZrMe})_2(\mu\text{-Me})^+\cdots(\text{C}_6\text{F}_5)_3\text{BCNB}(\text{C}_6\text{F}_5)_3]^-$ .**  $^1\text{H}$  NMR (300 MHz,  $\text{C}_6\text{D}_6$ , 298 K)  $\delta$  5.50 (s, 20H, Cp), -0.14 (s, 6H, Zr-Me), -1.40 (s, 3H,  $\mu\text{-Me}$ ).  **$\text{Cp}_2\text{ZrMe}(\mu\text{-Me})\text{B}(\text{C}_6\text{F}_5)_3$ .**<sup>42</sup>  $^1\text{H}$  NMR (300 MHz,  $\text{C}_6\text{D}_6$ , 298 K)  $\delta$  5.39 (s, 10H, Cp), 0.28 (s, 3H, Zr-Me), 0.1 (br, 3H, Zr-Me).  **$\text{Cp}_2\text{ZrMe}(\mu\text{-NC})\text{B}(\text{C}_6\text{F}_5)_3$ .**  $^1\text{H}$  NMR (300 MHz,  $\text{C}_6\text{D}_6$ , 298 K)  $\delta$  5.55 (s, 10H, Cp), 0.26 (s, 3H, Zr-Me).  **$\{[(\text{SBI})\text{ZrMe}]_2(\mu\text{-Me})^+\cdots(\text{C}_6\text{F}_5)_3\text{BCNB}(\text{C}_6\text{F}_5)_3\}^-$ .** From (SBI)ZrMe<sub>2</sub> (300  $\mu\text{L}$ , 0.004 mol/L) and **1** (250  $\mu\text{L}$ , 0.002 mol/L) in  $\text{C}_6\text{D}_6$ ,  $[\text{Zr}] = 0.0022 \text{ mol/L}$ .  $^1\text{H}$  NMR (300 MHz,  $\text{C}_6\text{D}_6$ , 298 K)  $\delta$  0.62 (s, 6H, Si-Me, *rac*-like), 0.59 (s, 6H, Si-Me, *meso*-like), 0.45 (s, 6H, Si-Me, *meso*-like), 0.42 (s, 6H, Si-Me, *rac*-like), -1.00 (s, 6H, Zr-Me, *rac*-like), -1.06 (s, 6H, Zr-Me, *meso*-like), -2.98 (s, 3H,  $\mu\text{-Me}$ , *rac*-like), -3.13 (s, 3H,  $\mu\text{-Me}$ , *meso*-like).  $^1\text{H}$  NMR (300 MHz,  $\text{CD}_2\text{Cl}_2$ , 223 K)  $\delta$  1.11 (s, 6H, Si-Me, *rac*-like), 1.03 (s, 6H, Si-Me, *meso*-like), 0.95 (s, 6H, Si-Me, *rac*-like), 0.94 (s, 6H, Si-Me, *meso*-like), -0.94 (s, 6H, Zr-Me, *meso*-like), -0.94 (s, 6H, Zr-Me, *rac*-like), -2.80 (s, 3H,  $\mu\text{-Me}$ , *rac*-like), -2.98 (s, 3H,  $\mu\text{-Me}$ , *meso*-like). Complete decomposition could only be detected after 24 h at 298 K. Mononuclear zirconocene cations were not detected.  **$(\text{SBI})\text{ZrMe}(\mu\text{-Me})\text{B}(\text{C}_6\text{F}_5)_3$ .**<sup>22</sup>  $^1\text{H}$  NMR (300 MHz,  $\text{C}_6\text{D}_6$ , 298 K)  $\delta$  6.57 (d, 1H,  $\alpha\text{-C}_5\text{H}_2$ , Zr-Me side), 6.22 (d, 1H,  $\alpha\text{-C}_5\text{H}_2$ , Me-B side), 5.66 (d, 1H,  $\alpha\text{-C}_5\text{H}_2$ , Me-B side), 4.97 (d, 1H,  $\alpha\text{-C}_5\text{H}_2$ ,

Zr-Me side), 0.34 (s, 3H,  $\text{Me}_2\text{Si}$ , Me-B side), 0.20 (s, 3H,  $\text{Me}_2\text{Si}$ , Zr-Me side), -0.44 (br, 3H, Me-B), -0.51 (s, 3H, Zr-Me).  **$(\text{SBI})\text{ZrMe}(\mu\text{-NC})\text{B}(\text{C}_6\text{F}_5)_3$ .**  $^1\text{H}$  NMR (300 MHz,  $\text{C}_6\text{D}_6$ , 298 K)  $\delta$  5.54 (d, 1H,  $\alpha\text{-C}_5\text{H}_2$ ), 5.09 (d, 1H,  $\alpha\text{-C}_5\text{H}_2$ ), 0.39 (s, 3H,  $\text{Me}_2\text{Si}$ ), 0.28 (s, 3H,  $\text{Me}_2\text{Si}$ ), -0.58 (s, 3H, Zr-Me).

**$\text{Cp}''_2\text{ZrMe}_2/\mathbf{1}/\text{AlMe}_3$ .** Into the NMR tube were weighed 15 mg of  $\text{Cp}''_2\text{ZrMe}_2$  ( $2.77 \times 10^{-5} \text{ mol}$ ) and 36 mg of **1** ( $2.78 \times 10^{-5} \text{ mol}$ ). To this mixture was added 14  $\mu\text{L}$  ( $2.8 \times 10^{-5} \text{ mol}$ ) of a toluene solution of  $\text{AlMe}_3$  (2 mol/L), followed by 0.5 mL pre-cooled ( $-78 \text{ }^\circ\text{C}$ )  $\text{CD}_2\text{Cl}_2$ ,  $[\text{Zr}] = 0.0554 \text{ mol/L}$ . On heating to room temperature the binuclear species proved stable in  $\text{CD}_2\text{Cl}_2$  for a few minutes, although decomposition was complete after  $\sim 10 \text{ min}$ .  **$[\text{Cp}''_2\text{Zr}(\mu\text{-Me})_2\text{AlMe}_2][\text{CN}\{\text{B}(\text{C}_6\text{F}_5)_3\}_2]^-$ .**  $^1\text{H}$  NMR (300 MHz,  $\text{CD}_2\text{Cl}_2$ , 223 K)  $\delta$  7.04 (s, 2H,  $\text{C}_5\text{H}_3$ ), 6.94 (s, 4H,  $\text{C}_5\text{H}_3$ ), 0.46 (s, 6H,  $\mu\text{-Me}$ ), 0.26 (s, 36H,  $\text{SiMe}_3$ ), -0.51 (s, 6H, AlMe) (the expected couplings of the Cp-signals are not resolved under these conditions).  $^{13}\text{C}$  NMR (75.5 MHz,  $\text{CD}_2\text{Cl}_2$ , 223 K)  $\delta$  128.6 (4C,  $\text{C}_5\text{H}_3$ ), 125.0 (2C,  $\text{C}_5\text{H}_3$ ), 37.9 ( $\mu\text{-Me}$ ), -0.4 ( $\text{SiMe}_3$ ), -6.7 (AlMe) (quaternary Cp carbons not detected).

**$\text{L}_2\text{ZrMe}_2/\mathbf{4c}$ .** A mixture of  $\text{Cp}_2\text{ZrMe}_2$  in  $\text{C}_6\text{D}_6$  (400  $\mu\text{L}$ , 0.004 mol/L) and **4c** in in  $\text{C}_6\text{D}_6/o\text{-C}_6\text{H}_4\text{F}_2$  (4:1) (100  $\mu\text{L}$ , 0.004 mol/L) gave exclusively the ion pair  $\{[(\text{Cp}_2\text{ZrMe})_2(\mu\text{-Me})^+\cdots\text{Ni}\{\text{CNB}(\text{C}_6\text{F}_5)_3\}_4]^{2-}\}$  ( $[\text{Zr}] = 0.0032 \text{ mol/L}$ ). Due to the higher polarity of the solvent mixture the signals for the cation show a low-field shift of up to 0.15 ppm compared to that in pure  $\text{C}_6\text{D}_6$ . Decomposition of  $\{[(\text{Cp}_2\text{ZrMe})_2(\mu\text{-Me})^+\cdots\text{Ni}\{\text{CNB}(\text{C}_6\text{F}_5)_3\}_4]^{2-}\}$  was complete after 60 min, while the SBI analogue showed only minor signs of decomposition after 30 min. In both cases  $\text{L}_2\text{ZrMe}(\mu\text{-Me})\text{B}(\text{C}_6\text{F}_5)_3$  was formed as the only detectable decomposition product.  **$[(\text{Cp}_2\text{ZrMe})_2(\mu\text{-Me})]_2[\text{Ni}\{\text{CNB}(\text{C}_6\text{F}_5)_3\}_4]$ .**  $^1\text{H}$  NMR (300 MHz,  $\text{C}_6\text{D}_6/o\text{-C}_6\text{H}_4\text{F}_2$  24:1, 298 K)  $\delta$  5.81 (s, 20H, Cp), 0.06 (s, 6H, Zr-Me), -1.11 (s, 3H,  $\mu\text{-Me}$ ).  **$\text{Cp}_2\text{ZrMe}(\mu\text{-Me})\text{B}(\text{C}_6\text{F}_5)_3$ .**  $^1\text{H}$  NMR (300 MHz,  $\text{C}_6\text{D}_6/o\text{-C}_6\text{H}_4\text{F}_2$  24:1, 298 K)  $\delta$  5.42 (s, 10H, Cp), 0.29 (s, 3H, Zr-Me), 0.15 (br, 3H, B-Me).  **$\{[(\text{SBI})\text{ZrMe}]_2(\mu\text{-Me})]_2[\text{Ni}\{\text{CNB}(\text{C}_6\text{F}_5)_3\}_4]$ .** From (SBI)ZrMe<sub>2</sub> in  $\text{C}_6\text{D}_6$  (400  $\mu\text{L}$ , 0.004 mol/L) and **4c** in in  $\text{C}_6\text{D}_6/o\text{-C}_6\text{H}_4\text{F}_2$  (4:1) (100  $\mu\text{L}$ , 0.004 mol/L),  $[\text{Zr}] = 0.0032 \text{ mol/L}$ .  $^1\text{H}$  NMR (300 MHz,  $\text{C}_6\text{D}_6/o\text{-C}_6\text{H}_4\text{F}_2$  24:1, 298 K)  $\delta$  -0.94 (s, 6H, Zr-Me, *meso*-like), -0.99 (s, 6H, Zr-Me, *rac*-like), -2.82 (s, 3H,  $\mu\text{-Me}$ , *rac*-like), -3.05 (s, 3H,  $\mu\text{-Me}$ , *meso*-like).

**Alkene Polymerizations.** Normal pressure polymerizations were performed in a flame-dried glass flask (250 mL for small scale reactions, 2 L for reactions with 1 L solvent volume) equipped with an efficient magnetic stirrer bar and an internal thermometer. The flask was evacuated, filled with monomer gas, followed by the required amount of toluene and triisobutyl aluminum (toluene solution,  $[\text{Al}] = 0.1 \text{ mol/L}$ ). Temperature equilibration was ensured by stirring the mixture on a water bath of the required temperature for  $\sim 10 \text{ min}$  (20 min for 1 L reactions). The required amount of a stock solution of the metallocene catalyst precursor in toluene (2  $\mu\text{mol/mL}$ ) was then injected using a gastight syringe with Teflon plunger, followed by the injection of the activator in toluene (1  $\mu\text{mol/mL}$ ). Polymerization times were measured from that point. The stirrer speed was 1200 rpm. All stock solutions were prepared freshly prior to polymerization runs and used within 2 h (usually within 30 min) to ensure consistent results. The polymerization was stopped by the rapid injection of 2 mL of methanol. The polymer was precipitated by pouring the contents of the flask into a large volume of acidified methanol, filtered and dried at 90  $^\circ\text{C}$  to constant weight.  $^{13}\text{C}$  NMR spectra of polymers were recorded in 1,2- $\text{C}_2\text{D}_2\text{Cl}_4$  at 110  $^\circ\text{C}$ .

For reactions under pressure, a 5 L Büchi stainless steel autoclave equipped with a pressure buret and connected to a Büchi gas flow controller was used. The reactor was heated out in vacuo at 100  $^\circ\text{C}$  (Julabo FP50 heater) for 2 h, allowed to cool, and charged with toluene (3L) via a wide-bore transfer cannula. The required aliquots of toluene solutions of  $\text{AlBu}_3$  and the metallocene were added, the pressure buret was charged with a toluene solution of the activator, and the autoclave was pressurized to 7 bar ethene pressure and allowed to equilibrate at 60  $^\circ\text{C}$  for 30 min. The buret was pressurized with argon (8 bar), and the activator injected rapidly with vigorous mechanical stirring. The reaction was terminated by the injection of 10 mL of methanol via the pressure buret, the reactor was vented, and the polymer was collected and worked up as described above.

(42) Yang, X.; Stern, C. L.; Marks, T. J. *J. Am. Chem. Soc.* **1994**, *116*, 10015.

**Table 7.** Crystal Data for Compounds **1**, **2**, **4b**

	<b>1</b>	<b>2</b>	<b>4b</b> ·2(CH <sub>3</sub> ) <sub>2</sub> CO
empirical formula	C <sub>56</sub> H <sub>15</sub> B <sub>2</sub> F <sub>30</sub> N	C <sub>37</sub> H <sub>15</sub> BClF <sub>15</sub>	C <sub>92</sub> H <sub>22</sub> B <sub>4</sub> F <sub>60</sub> N <sub>6</sub> Ni·2(CH <sub>3</sub> ) <sub>2</sub> CO
fw	1293.31	790.75	2569.26
temp (K)	150(2)	150(2)	150(2)
crystal size (mm)	0.6 × 0.36 × 0.18	0.51 × 0.33 × 0.24	0.30 × 0.18 × 0.18
crystal system	triclinic	monoclinic	triclinic
space group	<i>P</i> $\bar{1}$	<i>P</i> 2 <sub>1</sub> / <i>c</i>	<i>P</i> $\bar{1}$
<i>a</i> , Å	13.3342(2)	12.1402(2)	13.1128(3)
<i>b</i> , Å	14.8405(2)	7.91830(10)	13.9811(4)
<i>c</i> , Å	15.8631(2)	33.0914(4)	14.6945(3)
$\alpha$ , deg	116.4370(6)	90	116.1280(13)
$\beta$ , deg	90.9440(7)	99.3490(7)	93.7390(14)
$\gamma$ , deg	113.6410(5)	90	90.4300(12)
<i>V</i> , (Å <sup>3</sup> )	2501.10(6)	3138.81(8)	2411.55(10)
<i>Z</i>	2	4	1
<i>D</i> <sub>calcd</sub> (g cm <sup>−3</sup> )	1.717	1.673	1.769
$\mu$ , mm <sup>−1</sup>	0.178	0.241	0.374
<i>F</i> (000)	1276	1576	1268
max, min transmissn	0.9686 and 0.9005	0.9444 and 0.8869	0.9357 and 0.8961
$\theta$ range, deg	1.79 ≤ $\theta$ ≤ 26.00	2.27 ≤ $\theta$ ≤ 27.42	2.11 ≤ $\theta$ ≤ 26.00
index range	−16 ≤ <i>h</i> ≤ 16, −18 ≤ <i>k</i> ≤ 18, −19 ≤ <i>l</i> ≤ 19	−15 ≤ <i>h</i> ≤ 15, −10 ≤ <i>k</i> ≤ 10, −42 ≤ <i>l</i> ≤ 42	−16 ≤ <i>h</i> ≤ 16, −17 ≤ <i>k</i> ≤ 17, −18 ≤ <i>l</i> ≤ 18
no. of reflections collected	58348	73682	63405
no. of unique reflections, <i>n</i>	9800 ( <i>R</i> <sub>int</sub> = 0.0304)	7125 ( <i>R</i> <sub>int</sub> = 0.0800)	9478 ( <i>R</i> <sub>int</sub> = 0.0692)
no. of parameters, <i>p</i>	803	488	776
goodness of fit on <i>F</i> <sup>2</sup> , <i>s</i>	1.034	1.031	1.022
<i>R</i> <sub>1</sub> [ <i>I</i> > 2 $\sigma$ ( <i>I</i> )]	0.0355	0.0373	0.0409
<i>wR</i> <sub>2</sub> (all data)	0.0972	0.0895	0.1047
weighting parameters <i>a</i> , <i>b</i>	0.0394, 1.0052	0.0429, 1.2710	0.0435, 1.6787
extinction parameter	0.0048(11)	0.0022(5)	—
largest diff, peak, and hole e Å <sup>−3</sup>	0.507 and −0.257	0.429 and −0.325	0.806 and −0.357

<sup>a</sup> Definitions: *R*<sub>int</sub> = (Σ|*F*<sub>o</sub><sup>2</sup> − *F*<sub>o</sub><sup>2</sup> (mean)|Σ*F*<sub>o</sub><sup>2</sup>)/Σ*F*<sub>o</sub><sup>2</sup>; *S* = ((Σ*w*(*F*<sub>o</sub><sup>2</sup> − *F*<sub>c</sub><sup>2</sup>)/(*n* − *p*))<sup>1/2</sup>; *wR*<sub>2</sub> = ((Σ*w*(*F*<sub>o</sub><sup>2</sup> − *F*<sub>c</sub><sup>2</sup>)/Σ*w*(*F*<sub>o</sub><sup>2</sup>))<sup>1/2</sup>; *R*<sub>1</sub> = (Σ||*F*<sub>o</sub>| − |*F*<sub>c</sub>||/Σ|*F*<sub>o</sub>|); weighting scheme *w* = [ $\sigma^2(F_o^2) + (aP)^2 + bP$ ]<sup>−1</sup>, where *P* = [2*F*<sub>c</sub><sup>2</sup> + Max(*F*<sub>c</sub><sup>2</sup>, 0)]/3.

**Table 8.** Crystal Data for Compounds **4c**, **5c**, and **6**

	<b>4c</b> ·2CH <sub>2</sub> Cl <sub>2</sub>	<b>5c</b> ·2CH <sub>2</sub> Cl <sub>2</sub>	<b>6</b> ·C <sub>7</sub> H <sub>8</sub>
empirical formula	C <sub>114</sub> H <sub>30</sub> B <sub>4</sub> F <sub>60</sub> N <sub>4</sub> Ni·2CH <sub>2</sub> Cl <sub>2</sub>	C <sub>114</sub> H <sub>30</sub> B <sub>4</sub> F <sub>60</sub> N <sub>4</sub> Pd·2CH <sub>2</sub> Cl <sub>2</sub>	C <sub>42</sub> H <sub>45</sub> BF <sub>15</sub> NSi <sub>4</sub> Zr·C <sub>7</sub> H <sub>8</sub>
fw	2867.22	2914.92	1155.31
temp (K)	150(2)	150(2)	150(2)
crystal size (mm)	0.36 × 0.15 × 0.12	0.69 × 0.42 × 0.38	0.24 × 0.24 × 0.09
crystal system	monoclinic	monoclinic	triclinic
space group	<i>P</i> 2 <sub>1</sub> / <i>c</i>	<i>P</i> 2 <sub>1</sub> / <i>c</i>	<i>P</i> $\bar{1}$
<i>a</i> , Å	12.03400(10)	12.01790	11.9439(5)
<i>b</i> , Å	14.62970(10)	14.7304(3)	12.9731(5)
<i>c</i> , Å	31.8468(3)	31.88720(3)	18.9530(6)
$\alpha$ , deg	90	90	77.677(2)
$\beta$ , deg	100.6920(6)	100.2870	74.010(2)
$\gamma$ , deg	90	90	75.461(2)
<i>V</i> , (Å <sup>3</sup> )	5509.41(8)	5551.55(15)	2699.7(2)
<i>Z</i>	2	2	2
<i>D</i> <sub>calcd</sub> (g cm <sup>−3</sup> )	1.728	1.744	1.421
$\mu$ , mm <sup>−1</sup>	0.430	0.419	0.378
<i>F</i> (000)	2828	2864	1180
max, min transmissn	0.9503 and 0.8607	0.9503 and 0.8607	0.9668 and 0.9147
$\theta$ range, deg	2.40 ≤ $\theta$ ≤ 26.00	2.40 ≤ $\theta$ ≤ 26.00	2.12 ≤ $\theta$ ≤ 26.00
index range	−14 ≤ <i>h</i> ≤ 14, −18 ≤ <i>k</i> ≤ 18, −39 ≤ <i>l</i> ≤ 39	−14 ≤ <i>h</i> ≤ 14, −18 ≤ <i>k</i> ≤ 18, −39 ≤ <i>l</i> ≤ 39	−13 ≤ <i>h</i> ≤ 14, −15 ≤ <i>k</i> ≤ 15, −22 ≤ <i>l</i> ≤ 23
no. of reflections collected	114737	31285	37640
no. of unique reflections, <i>n</i>	10807 ( <i>R</i> <sub>int</sub> = 0.0419)	10818 ( <i>R</i> <sub>int</sub> = 0.0552)	10561 ( <i>R</i> <sub>int</sub> = 0.0672)
no. of parameters, <i>p</i>	854	854	655
goodness of fit on <i>F</i> <sup>2</sup> , <i>s</i>	1.006	1.026	1.102
<i>R</i> <sub>1</sub> [ <i>I</i> > 2 $\sigma$ ( <i>I</i> )]	0.0344	0.0393	0.0455
<i>wR</i> <sub>2</sub> (all data)	0.0857	0.1042	0.1096
weighting parameters <i>a</i> , <i>b</i>	0.0376, 3.1149	0.0487, 3.9774	0.0370, 1.5817
extinction parameter	0.00045(14)	0.0010(4)	0.0121(10)
largest diff, peak, and hole e Å <sup>−3</sup>	0.527 and −0.422	0.602 and −0.709	0.684 and −0.520

<sup>a</sup> Definitions: *R*<sub>int</sub> = (Σ|*F*<sub>o</sub><sup>2</sup> − *F*<sub>o</sub><sup>2</sup> (mean)|Σ*F*<sub>o</sub><sup>2</sup>)/Σ*F*<sub>o</sub><sup>2</sup>; *S* = ((Σ*w*(*F*<sub>o</sub><sup>2</sup> − *F*<sub>c</sub><sup>2</sup>)/(*n* − *p*))<sup>1/2</sup>; *wR*<sub>2</sub> = ((Σ*w*(*F*<sub>o</sub><sup>2</sup> − *F*<sub>c</sub><sup>2</sup>)/Σ*w*(*F*<sub>o</sub><sup>2</sup>))<sup>1/2</sup>; *R*<sub>1</sub> = (Σ||*F*<sub>o</sub>| − |*F*<sub>c</sub>||/Σ|*F*<sub>o</sub>|); weighting scheme *w* = [ $\sigma^2(F_o^2) + (aP)^2 + bP$ ]<sup>−1</sup>, where *P* = [2*F*<sub>c</sub><sup>2</sup> + Max(*F*<sub>c</sub><sup>2</sup>, 0)]/3.

**X-ray Crystallography.** In each case a suitable crystal was coated in an inert perfluoropolyether oil and mounted in a nitrogen stream at

150 K on a Nonius Kappa CCD area-detector diffractometer. Data collection was performed using Mo K $\alpha$  radiation ( $\lambda$  = 0.710 73 Å)

with the CCD detector placed 30 mm from the sample via a mixture of  $1^\circ \phi$  and  $\omega$  scans at different  $\theta$  and  $\kappa$  settings using the program COLLECT.<sup>43</sup> The raw data were processed to produce conventional data using the program DENZO-SMN.<sup>44</sup> The datasets were corrected for absorption using the program SORTAV.<sup>45</sup> All structures were solved by heavy-atom methods using SHELXS-97<sup>46</sup> and were refined by full-matrix least squares refinement (on  $F^2$ ) using SHELXL-97.<sup>47</sup> All non-

(43) Collect, data collection software, Nonius, B. V.: Delft, The Netherlands, 1999.

(44) Otwinowski Z.; Minor, W. In *Methods in Enzymology*; Carter, C. W., Jr., Sweet, R. M., Eds.; Academic Press: New York, 1996; pp 276, 307.

(45) Blessing, R. H. *Acta Crystallogr., Sect. A* **1995**, *51*, 33.

(46) Sheldrick, G. M. *Acta Crystallogr., Sect. A* **1990**, *46*, 467.

(47) Sheldrick, G. M. *SHELXL-97*, Program for crystal structure refinement. University of Göttingen: Germany, 1997.

hydrogen atoms were refined with anisotropic displacement parameters. Hydrogen atoms were constrained to idealized positions. Crystallographic data for compounds **1**, **2**, **4b**·Me<sub>2</sub>CO, **4c**·2CH<sub>2</sub>Cl<sub>2</sub>, **5c**·2CH<sub>2</sub>Cl<sub>2</sub>, and **6**·toluene are summarized in Tables 7 and 8.

**Acknowledgment.** This work was supported by the Engineering and Physical Sciences Research Council and the University of Leeds.

**Supporting Information Available:** Details of crystal structure determinations for compounds **1**, **2**, **4b**, **4c**, **5c**, and **6** (PDF). This material is available free of charge via the Internet at <http://pubs.acs.org>.

JA002820H